Phototactic Migration of *Dictyostelium* Cells Is Linked to a New Type of Gelsolin-related Protein

Susanne Stocker, Mary Hiery, and Gerard Marriott*

Max-Planck-Institute for Biochemistry, D-82152 Martinsried, Germany

The molecular and functional characterization of a 125-kDa Ca^{2+}-extractable protein of the Triton X-100–insoluble fraction of *Dictyostelium* cells identified a new type of a gelsolin-related molecule. In addition to its five gelsolin segments, this gelsolin-related protein of 125 kDa (GRP125) reveals a number of unique domains, two of which are predicted to form coiled-coil regions. Another distinct attribute of GRP125 concerns the lack of sequence elements known to be essential for characteristic activities of gelsolin-like proteins, i.e. the severing, capping, or nucleation of actin filaments. The subcellular distribution of GRP125 to vesicular compartments suggests an activity of GRP125 different from actin-binding, gelsolin-related proteins. GRP125 expression is tightly regulated and peaks at the transition to the multicellular pseudoplasmodial stage of *Dictyostelium* development. GRP125 was found indispensable for slug phototaxis, because slugs fail to correctly readjust their orientation in the absence of GRP125. Analysis of the GRP125-deficient mutant showed that GRP125 is required for coupling photodetection to the locomotory machinery of slugs. We propose that GRP125 is essential in the natural environment for the propagation of *Dictyostelium* spores. We also present evidence for further representatives of the GRP125 type in *Dictyostelium*, as well as in heterologous cells from lower to higher eukaryotes.

INTRODUCTION

A number of basic cellular functions require a rapid, localized reorganization of the actin cytoskeleton, and Ca^{2+}-sensitive microfilament proteins often hold a key position in the regulation of these processes (Brundage *et al.*, 1993). Triton X-100 treatment of cells solubilizes a substantial proportion of intracellular proteins, whereas the insoluble fraction is enriched in cytoskeletal proteins (Prassler *et al.*, 1998). The Ca^{2+} extract of the Triton X-100–insoluble cellular material harbors a valuable source of structural and regulatory proteins of the actin cytoskeleton (Jungbluth *et al.*, 1995; Prassler *et al.*, 1997, 1998). This Ca^{2+} extract was further screened as part of our continuing efforts to identify and characterize proteins involved in the regulation of the organization and dynamics of the actin cytoskeleton. In this study we describe a previously uncharacterized 125-kDa protein identified in the Ca^{2+} extract that has several hallmarks of the gelsolin

family of actin-binding proteins. We therefore refer to this protein as gelsolin-related protein of 125 kDa (GRP125).

Gelsolin-related proteins are characterized by repeats of 125–150 amino acid segments constituting clusters of conserved sequence motifs that define a characteristic three-dimensional domain structure (Way and Weeds, 1988, McLaughlin *et al.*, 1993) (compare Figure 1A). These segments in gelsolin-related proteins are organized in triplicate, reflecting a gene multiplication of a prototypical "gelsolin domain" (Kwiatkowski *et al.*, 1986, Bazari *et al.*, 1988). Members of the gelsolin family typically exist as either three-domain proteins, such as severin from *Dictyostelium discoideum* (Yamamoto *et al.*, 1982), fragmin from *Physarum* (Hasegawa *et al.*, 1980), and capG (in macrophages and fibroblasts [Southwick and DiNubile, 1986]), or six-domain proteins, such as adseverin (in adrenal glands [Maekawa *et al.*, 1989]) and gelsolin (Yin and Stossel, 1979). Gelsolin is expressed in most mammalian cell lines (Kwiatkowski *et al.*, 1988a,b), and gelsolin homologues have been identified in *Dro-*

* Corresponding author.
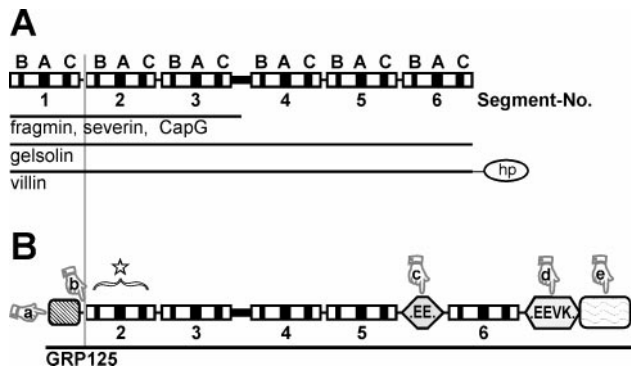
Figure 1. Comparison of GRP125 with members of the gelsolin family of actin-binding proteins. (A) Domain organization of gelsolin-related proteins that comprise three (fragmin, severin, and capG) or six segmental repeats (gelsolin, villin [hp, headpiece]). Each segment contains conserved motifs, labeled B, A, and C (modified from Way and Weeds, 1988). (B) Scheme of GRP125 presenting repeats and motifs according to A. N- and C-terminal repetitive regions of GRP125 are highlighted as rectangles; the repetitive, glutamate-rich regions are highlighted as hexagons. The star symbolizes the presence of gelsolin segments in GRP125; the pointers mark unique features of GRP125: (a) first gelsolin segment is missing; (b) PIP$_2$– and F-actin–binding motifs conserved only partially; (c and d) glutamate-rich regions; (a and e) repetitive N- and C-terminal extensions.

sophila (Heintzelmann *et al.*, 1993), *Xenopus* (Ankenbauer *et al.*, 1989), earthworm (D'Haese and Hinssen, 1987), and different crustaceae (Lück *et al.*, 1995).

Interestingly, some gelsolin relatives integrate the typical activities of gelsolin-family members—capping, severing, and nucleation of actin filaments—with other interactions or activities mediated by additional domains. The well-characterized villin protein (Bretscher and Weber, 1980) exhibits a C-terminal headpiece, which harbors an additional F-actin–binding site that is used to form tightly packed actin bundles (Glenney and Weber, 1981). On the other hand, a *myc* basic homology region in CapG (Prendergast and Ziff, 1991), as well as an N-terminal extension of the recently described supervillin (Pestonjamasp *et al.*, 1997), might be involved in the nuclear localization of these proteins. Finally, the flightless I gene product of *Drosophila* contains a leucine-rich repeat at its N terminus, a domain known to mediate protein–protein interactions (Campbell *et al.*, 1993).

A sequence-based characterization of GRP125 conducted in this study reveals unique N-and C-terminal domains in addition to its gelsolin core. Mutant cells lacking GRP125 exhibit a defect in their phototactic response in that photodetection is uncoupled from the locomotory machinery. The identification of GRP125 as a new type of gelsolin-related protein extends the structural and functional characteristics of the gelsolin protein family.

MATERIALS AND METHODS

Cell Culture and Development of Dictyostelium Cells

The *D. discoideum* strain AX2 and GRP125-null mutants were cultivated at 23°C in shaken suspension (150 rpm; Claviez *et al.*, 1982) using axenic nutrient medium or else were grown in medium on Petri dishes. To analyze development to aggregation competence, cells were washed and resuspended in 17 mM K-Na phosphate buffer (pH 6.0) at 10^7 cells/ml and shaken at 150 rpm for 9 h. In addition, analysis of developmental regulation was accomplished by developing 5×10^7 cells on nitrocellulose filters (Newell *et al.*, 1969). Cells at different developmental stages were scraped off filters using a razor blade and lysed in Tris-HCl (pH 7.5), 0.1% SDS, 1 mM DTT, 1 mM Pefabloc (Boehringer Mannheim, Mannheim, Germany), and 1% protease inhibitor mixture (antipain, bestatin A, leupeptin, pepstatin, 10 µg/ml each) for preparation of total protein (Furukawa *et al.*, 1992). Growth and development were also examined using cells grown on nutrient agar plates on a lawn of *Escherichia coli* B/2 (Noegel *et al.*, 1985). NIH/3T3 fibroblasts were grown on HCl-treated, poly-L-lysine–coated glass coverslips in DMEM supplemented with 10% FCS and 1% penicillin/streptomycin and processed for microinjection as described by Celis (1994) (cell culture material purchased from Life Technologies, Gaithersburg, MD).

Phototaxis experiments were performed essentially as described by Wallraff (1997). Up to 1×10^7 AX2 or mutant cells were applied onto the surface of a water agar plate 9 cm in diameter. The application point was asymmetrically located to one side of the plate, and its distance to the light port was 7.5 cm. Control experiments conducted in the absence of light used cells applied to the center of the plate. After incubation for 3 d at 23°C in a phototaxis chamber, trails and cellular material were blotted to noncoated transparencies and stained with Coomassie Blue. For analysis of the phototactic response of *Dictyostelium* fruiting bodies, nutrient agar plates containing a lawn of *E. coli* B/2 cells were point inoculated with the *D. discoideum* strain AX2 or the GRP125-null mutants, incubated for 4 d in the phototaxis chamber, and photographed from above.

Cloning, Sequencing, and Analysis of the GRP125 Coding Region

A λgt11 cDNA expression library prepared from *D. discoideum* AX3 cells starved for 4 h (Clontech Laboratories, Palo Alto, CA) was screened with the ^{125}I-labeled monoclonal antibody (mAb) 212-174-1 (see below). This screen identified a 2.5-kb clone, λ-1A, which corresponds to a fragment of the GRP125 coding sequence from bp 205 to 2727 (A of ATG = 1). A genomic map was constructed using ^{32}P-labeled parts of the 2.5-kb phage clone at its 5′ (probe F3, bp 205–625 of the GRP125 coding region) and 3′ ends (probe F1, bp 1228–2727). A 2.7-kb *Eco*RI fragment at the 5′ end and a 2.8-kb *Eco*RI fragment at the 3′ end of λ-1A were found appropriate for inverted PCR amplification and thus to compile the complete sequence of GRP125. Eight micrograms of genomic *D. discoideum* AX2 DNA were digested with *Eco*RI and religated in an ample volume. A 100-µl reaction mixture for inverted PCR contained 0.2 µg of this template and 0.1-nM primers (3′-GCG AAG CTT GCA TCA CTT TGC ATA ATG AAA ACA TCC and 5′-GCG GGA TCC GAA TGA TAT ATT CCA AGT TGA CG for amplification of the 5′ fragment and 3′-GCG AAG CTT CGA CGG GAT CAT CTG ATT TC and 5′-GCG GGA TCC GGT CAA TGA CGA AGC CAC CG for amplification of the 3′ fragment). Temperature cycles started with 3 min at 96°C, followed by 30 cycles of 94°C for 1 min, 58°C for 1 min, 72°C for 3 min, and finally 5 min at 72°C. Primers were designed to obtain a *Bam*HI site at the 5′ end and a *Hind*III site at the 3′ end of the amplified product, which was cloned into pIC20R (Marsh *et al.*, 1984). Three independent clones were sequenced for the amplification product at the 3′ end (bp 2482–3992 of the GRP125 coding

region). The sequence of the amplified product at the 5' end (-1733–293) was verified by sequencing a clone identified with the 5' probe (probe F3, bp 205–625 of the GRP125 coding region) in a screen of a genomic *D. discoideum* AX3 plasmid library (courtesy of R.A. Firtel, University of California, San Diego, La Jolla, CA). This clone, G5, includes ~6.5 kb upstream of the grp125 gene until bp 2051 of the GRP125 coding sequence. Sequencing of DNA double strands was generally performed in both directions with uni, reverse, and sequence-specific primers applying the chain termination method (Sanger *et al.*, 1977), or the dye termination method on an ABI fluorescent sequencer (Applied Biosystems, Perkin Elmer-Cetus, Norwalk, CT). Programs bestfit, coilscan, fasta, gap, motifs, peptidesort, and pileup of the Wisconsin Package Version 9.1 (Genetics Computer Group, Madison, WI) and blastp 2.0.3 (Altschul *et al.*, 1997) were used to analyze the GRP125 sequence. Coiled-coil predictions were compared applying a window size of 21 and MTK and MTIK matrices with and without weighting options (MTK, matrix derived from the sequences of myosins, tropomyosins and keratins [intermediate filaments type I and II]; Lupas *et al.*, 1991; MTIDK, matrix derived from myosins, paramyosins, tropomysins, intermediate filaments type I–V, desmosomal proteins, and kinesins; Lupas, 1996).

Expression of GRP125 Polypeptide Fragments

A cDNA fragment coding for residues Asp-60 to Leu-308 of GRP125 (corresponding to S2 and S3 of GRP125) was obtained by PCR using primers designed to introduce a *Bam*HI site at the 5' end and a *Hin*dIII site at the 3' end. The amplified product was cloned into the expression vector pQE30 (Qiagen, Chatsworth, CA) and, after sequence verification, expressed in *E. coli* M15. The His-tagged GRP125 fragment, designated GRP125/S2S3, was purified after isopropyl-1-thio-β-D-galactopyranoside induction for 1 h from the soluble fraction of bacterial extracts on nickel-nitrilotriacetic acid-agarose as recommended by the manufacturer (Qiagen). For microinjection of GRP125/S2S3 into NIH/3T3 fibroblasts, the polypeptide was fluorescently labeled in 20 mM phosphate buffer (pH 7.8) using tetramethylrhodamine iodoacetamide (Molecular Probes, Eugene, OR) as described by Marriott (1994). Additionally, an *Eco*RI cDNA fragment coding for residues Glu-181 to Ser-380 of GRP125 (corresponding to S3 and most of S4 of GRP125) was cloned into the pIMS5 expression vector (Simon *et al.*, 1988) and expressed in *E. coli* JM105. Lysis of bacteria was achieved in 10 mM Tris-HCl (pH 8.0), 100 mM NaCl, 1 mM DTT, 5 mM EDTA, 0.5 mM Pefabloc, and 1% protease inhibitors (see above) using a French press (Aminco; Spectronic Instruments, Rochester, NY) at 16,000 psi. The lysate was centrifuged at $13,000 \times g$, and the recombinant polypeptide, GRP125/S3S4, was isolated from the pelleted inclusion bodies in sufficient purity after several wash steps. Thus, the first wash was accomplished by adding to the above-mentioned buffer 1 mM EGTA, 25% sucrose, and 1% Triton X-100. Subsequent wash steps applied increasing amounts of urea (0, 2, and 4 M) in 10 mM Tris-HCl (pH 8.0), 100 mM NaCl, 1 mM DTT, 1 mM EGTA, 0.5 mM Pefabloc, and 1% protease inhibitors. Solubilization of GRP125/S3S4 occurred at the 6 M urea extraction step; refolding of GRP125/S3S4 was achieved by gradually removing the urea by dialysis.

Gene Replacement in D. discoideum

For the construction of the targeting vector a genomic DNA fragment comprising bp -81–1739 of the GRP125 coding region was obtained by PCR using primers 5'-GTG TGT ATC ATT AAA ATT G and 3'-CAA TAT CAT TAG AAT TAC C. The amplified product was cloned into the pGEMT vector (Promega, Madison, WI). Because of the absence of *Eco*RI sites in its multiple cloning sites, a central genomic 5'-*Eco*RI-3'-*Eco*RI fragment was readily deleted via restriction with *Eco*RI and isolation of the vector-containing moiety. This latter fragment was blunt end ligated to the 1.4-kb Bsr cassette, which had been excised from plasmid pBsr2 (Sutoh, 1993) using

*Xba*I and *Hin*dIII. The construct was isolated with *Not*I–*Nco*I, dephosphorylated, and used to transfect *D. discoideum* AX2 cells by electroporation (Celis, 1994). Transformants were selected with 7.5 μg/ml blasticidin S (Calbiochem-Novabiochem, San Diego, CA) in nutrient medium, and independent clones of the GRP125-null mutants were isolated (Wallraff and Gerisch, 1991).

Antibody Production

mAb 212-174-1 was obtained from a BALB/c mouse immunized intraperitoneally with a Ca^{2+} extract preparation and Freund's adjuvant (Celis, 1994). This Ca^{2+} extract was isolated from Triton X-100–insoluble cell fractions of *Dictyostelium* as described by Prassler *et al.* (1997). Spleen cells were fused with PAIB₃ag8I-myeloma cells. Antibody 212-174-1 was identified in hybridoma culture supernatant by immunofluorescent labeling as well as comparative immunoblot analysis of the Ca^{2+} extract and of homogenates from *D. discoideum* cells. Polyclonal antibodies directed against S2 and S3 of GRP125 were raised in a rabbit by subcutaneous immunization with the recombinant His-tagged GRP125/S2S3 fragment applying a standard immunization protocol that used Freund's adjuvant. The serum was affinity purified on GRP125/S2S3 covalently linked to a 6-aminohexanoic acid *N*-hydroxysuccinimide ester-Sepharose column (Pharmacia, Uppsala, Sweden). Bound antibodies were eluted with 100 mM glycine (pH 2.4) and dialyzed against PBS. Similarly, polyclonal antibodies directed against S3 and S4 of GRP125 were raised by injecting a rabbit with the GRP125/S3S4 fragment using Hunter's TiterMax (Sigma, Deisenhofen, Germany) as adjuvant. The serum was affinity purified as described above on GRP125/S3S4 coupled to a 6-aminohexanoic acid *N*-hydroxysuccinimide ester-Sepharose column.
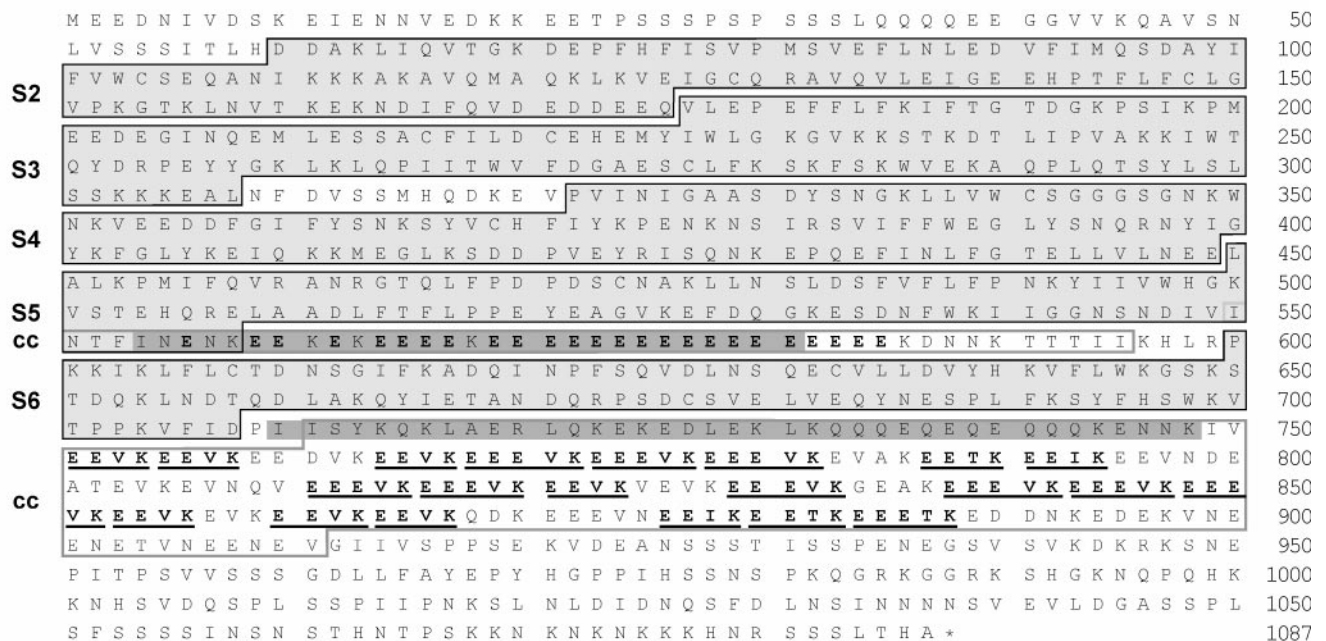
Immunofluorescence

For immunofluorescence labeling, growth phase or aggregation-competent *Dictyostelium* cells were allowed to adhere to glass coverslips 40 min before fixation. Cells were either fixed for 10 min with cold methanol at $-20°C$ or fixation was accomplished with picric acid/formaldehyde and a postfixation step in 70% ethanol (Humbel and Biegelmann, 1992). Binding of anti-GRP125 polyclonal antibodies was detected with Cy3-conjugated goat anti-rabbit immunoglobulin G (IgG; Jackson ImmunoResearch Laboratories, West Grove, PA). Imaging of cells was achieved using an Axiovert 135 fluorescence microscope equipped with a Plan Neofluar 100× oil objective (Zeiss, Oberkochen, Germany) and a cooled charge-coupled device camera (NU200; Photometrics, Tucson, AZ).

Miscellaneous

For Southern blots, genomic DNA of *D. discoideum* was prepared as described by Noegel *et al.* (1985) and, after restriction, transferred to nylon membranes (Biodyne B; Pall Biodyne, East Hills, NY). Fragments of the cDNA clone λ-1A comprising bp 205–640 (F3), 635-1234 (F2), or 1228–2727 (F1) of the GRP125 coding region or the Bsr encoding sequence were nick translated and used as probes for hybridization experiments in the presence of 30% formamide. Subsequent wash steps used low-stringency (30% formamide), medium-stringency (40% formamide), and high-stringency (50% formamide) conditions. SDS-PAGE was performed on 3–20% gradient gels or 10% minigels using the buffer system described by Laemmli (1970). For Western blotting, proteins were transferred to nitrocellulose (Towbin *et al.*, 1979). Mouse anti-cap34 (Hartmann *et al.*, 1989), mouse anti-actin (Simpson *et al.*, 1984), or mouse anti-csA (Bertholdt *et al.*, 1985) were detected using iodinated sheep anti-mouse IgG (Amersham Buchler, Braunschweig, Germany). Detection of polyclonal rabbit anti-GRP125 antibodies was achieved with iodinated goat anti-rabbit IgG prepared by the chloramine-T method (Sambrook *et al.*, 1989). Labeling intensity was quantified with a Fuji BAS 1000 bioimaging analyzer (Phosphoimager; Fuji

A


```
      M E E D N I V D S K  E I E N N V E D K K  E E T P S S S P S P  S S S L Q Q Q Q E E  G G V V K Q A V S N    50
      L V S S S I T L H D  D A K L I Q V T G K  D E P F H F I S V P  M S V E F L N L E D  V F I M Q S D A Y I   100
S2    F V W C S E Q A N I  K K K A K A V Q M A  Q K L K V E I G C Q  R A V Q V L E I G E  E H P T F L F C L G   150
      V P K G T K L N V T  K E K N D I F Q V D  E D D E E Q V L E P  E F F L F K I F T G  T D G K P S I K P M   200
      E E D E G I N Q E M  L E S S A C F I L D  C E H E M Y I W L G  K G V K K S T K D T  L I P V A K K I W T   250
S3    Q Y D R P E Y Y G K  L K L Q P I I T W V  F D G A E S C L F K  S K F S K W V E K A  Q P L Q T S Y L S L   300
      S S K K K E A L N F  D V S S M H Q D K E  V P V I N I G A A S  D Y S N G K L L V W  C S G G G S G N K W   350
S4    N K V E E D D F G I  F Y S N K S Y V C H  F I Y K P E N K N S  I R S V I F F W E G  L Y S N Q R N Y I G   400
      Y K F G L Y K E I Q  K K M E G L K S D D  P V E Y R I S Q N K  E P Q E F I N L F G  T E L L V L N E E L   450
      A L K P M I F Q V R  A N R G T Q L F P D  P D S C N A K L L N  S L D S F V F L F P  N K Y I I V W H G K   500
S5    V S T E H Q R E L A  A D L F T F L P P E  Y E A G V K E F D Q  G K E S D N F W K I  I G G N S N D I V I   550
CC    N T F I N E N K E E  K E K E E E E K E E  E E E E E E E E E E  E E E E K D N N K  T T T I I K H L R P   600
      K K I K L F L C T D  N S G I F K A D Q I  N P F S Q V D L N S  Q E C V L L D V Y H  K V F L W K G S K S   650
S6    T D Q K L N D T Q D  L A K Q Y I E T A N  D Q R P S D C S V E  L V E Q Y N E S P L  F K S Y F H S W K V   700
      T P P K V F I D P I  I S Y K Q K L A E R  L Q K E K E D L E K  L K Q Q Q E Q E Q E  Q Q Q K E N N K I V   750
      E E V K E E V K E E  D V K E E V K E E E  V K E E V K E E E  V K E V A K E E T K  E E I K E E V N D E   800
      A T E V K E V N Q V  E E E V K E E E V K  E E V K V E V K E E  E V K G E A K E E E  V K E E V K E E E   850
CC    V K E E V K E V K E  E V K E E V K Q D K  E E E V N E E I K E  E T K E E E T K E D  D N K E D E K V N E   900
      E N E T V N E E N E  V G I I V S P P S E  K V D E A N S S S T  I S S P E N E G S V  S V K D K R K S N E   950
      P I T P S V V S S S  G D L L F A Y E P Y  H G P P I H S S N S  P K Q G R K G G R K  S H G K N Q P Q H K  1000
      K N H S V D Q S P L  S S P I I P N K S L  N L D I D N Q S F D  L N S I N N N N S V  E V L D G A S S P L  1050
      S F S S S S I N S N  S T H N T P S K K N  K N K N K K K H N R  S S S L T H A *                         1087
```

Figure 2. (A) GRP125's gelsolin-like segments (S) and repetitive glutamate-rich regions. Black frames indicate segment borders (Way and Weeds, 1988; Eichinger and Schleicher, 1992; Hofmann, 1994). Glutamate-rich stretches are highlighted in bold; the (E)EEV[I,T]K motifs are underlined. Gray shading is applied to coiled-coil regions (cc) predicted with weighting of heptad positions *a* and *d*. Gray frames outline coiled-coil regions according to predictions without weighting options. (B) Alignment of motifs (see A) conserved in all domains of gelsolin family members. DGS, *Drosophila* gelsolin (Heintzelmann *et al.*, 1993); PGS, pig plasma gelsolin (Way and Weeds, 1988); VIL, chicken villin (Bazari *et al.*, 1988); DPV, *Dictyostelium* protovillin (Hofmann *et al.*, 1993); SVL, bovine supervillin (Pestonjamasp *et al.*, 1997); FRA, fragmin from *Physarum* (Ampe *et al.*, 1987); SEV, severin from *Dictyostelium* (André *et al.*, 1988); FLI, human flightless I homologue (Campbell *et al.*, 1993); aa-no., amino acid number (modified from Bazari *et al.*, 1988; Way and Weeds, 1988; Heintzelmann *et al.*, 1993). (C) Presence and conservation of motifs at the S1–S2 border in gelsolin-related proteins involved in PIP$_2$ binding (Yu *et al.*, 1992), severing of actin filaments (Kwiatkowski *et al.*, 1989), and F-actin binding (Sun *et al.*, 1994). h-pgs, human plasma gelsolin (Kwiatkowski *et al.*, 1986); h-vil, human villin (Arpin *et al.*, 1988); d-pvl, protovillin from *Dictyostelium* (Hofmann *et al.*, 1993).

Photo Film, Tokyo, Japan). Cell and tissue homogenates of diverse origin for the "Zoo-Blot" were provided by B. Muehlbauer and G. Gerisch (Max-Planck-Institute for Biochemistry). The concentration of proteins was determined according to Bradford (1976) referring to bovine IgG as standard.

RESULTS

Identification of a 125-kDa Protein in the Ca^{2+} Extract of the Triton X-100–insoluble Cellular Fraction

In an effort to identify and analyze regulatory microfilament components present in the Ca^{2+}-extract of the Triton X-100-insoluble cellular material of *D. discoideum*, mAbs were generated against this fraction and used to screen a λgt11 expression library of *D. discoideum* cDNA. mAb 212-174-1 identified a cDNA fragment of 2.5 kb truncated at its 5' and 3' ends. Application of inverted PCR techniques and further analysis of a genomic library using the initial phage clone as a probe yielded the sequence of a complete open reading frame. The coding sequence from the ATG start to the TAA stop codon comprises 3358 bp. There are two exons (409 and 2852 nucleotides), separated by a short intron of 94 bp, that encode a polypeptide 1087 amino acids in length (Figure 2A). The protein product of this gene has a predicted relative molecular mass of 124,777 and a calculated pI of 4.55, which evidently reflects the high content of glutamate residues (Figure 2A).

Sequence Analysis Identified GRP125 as a Member of the Gelsolin Family of Actin-binding Proteins

Analysis of the deduced amino acid sequence of the 125-kDa polypeptide revealed a significant similarity to members of the gelsolin family of actin-binding proteins. It displayed an overall identity to human plasma gelsolin of 27% with a 48% similarity (Kwiatkowski *et al.*, 1988a). We therefore designate this polypeptide GRP125, gelsolin-related protein of 125 kDa. Consistent with this categorization, GRP125 revealed a segmental organization typical of members of the gelsolin family (Figure 1, A and B). The highly

B

```
Sequence Segment AA-No. |----- Motif B -----| AA-No. |-------- Motif A --------| AA-No. |------ Motif C ------|

PGS       2    167   F NRG D C FIL   181   I YQ W C G SNSNRY E RLK A   220   ED A EP AG ML Q VL
DGS       2    207   M NTG D C FIL   221   I YV W V G SQAKRV E KLK A   263   TD A DK QH FF D VL
VIL       2    159   F NLG D V FLL   173   I IQ W N G PESNRA E RLR A   215   EA A SP -E LM Q AL
DPV       2    216   L NSG D V FLL   230   I YQ W N G SESSRL E KGK G   272   DK D HP -E FW K RL
SVL       2   1044   L NSG D C FLL  1058   C FL W V G EVANVI E KAK A  1105   TH A AK -D FW K LL
FRA       2    189   L NSG D V FVL   203   V IQ W N G AKAGLL E KVK A   242   AD N DT -E FF T LL
SEV       2    184   L NSG D C FLL   198   I YQ F N G SKSSPQ E KNK A   238   DS D IP AE FW K LL
FLI       2    642   L DPR F V FLL   656   I YV W R G AQATLS S TTK A   696   GQ E LP -E FW E AL
GRP125    2     86   L NLE D V FIM   100   I FV W C S EQANIK K KAK A   138   IG E EH PT FL F CL

PGS       3    283   L KSE D C FIL   299   I FV W K G KQANTE E RKA A   339   EG G ET PL FK Q FF
DGS       3    329   L DTR E C FIL   343   I FV W V G KGATQK E KTD A   383   EG S ES AP FK Q YF
VIL       3    279   L QHE D V YIL   294   I FV W K G KNANKE E KQQ A   335   DG S AV FR Q LF
DPV       3    338   L NAE F C YIL   352   L YV W L G KASAND Q RTV A   392   QG S EN TL FK DK FK
SVL       3   1167   L QSK E V LVF  1181   V YV W H G KEVTLA Q RKI A  1246   EH N ET IL FK EK FL
FRA       3    282   L DSN D V FVL   319   V FA W V G KHASVG E KKK A   359   EG G EN EV EF ED FF
SEV       3    295   L KSE D V FII   309   I YT W I G SKSSPN E KKT A   349   EN G TN QS FE T LL
FLI       3    770   L DTR C V YIL   784   V FI W L G RKSPRL V RAA L   824   EG T EA QV FK AK FK
GRP125    3    211   L ESS A C FIL   225   M YI W L G KGVKKS T KDT L   272   DG A ES CL FK SK FS

PGS       4    425   F YGG D S YII   447   I YN W Q G AQSTQD E VAA S   485   QG K EP AH LM S LF
DGS       4    479   L LGF A S YVL   502   T YV W H G VKASAA A RKR A   536   QG H EP RH FY K IF
XGS       4    104   F YGG D S YVL   126   I YT W Q G DDSTQD E ITA S   164   QG K EP AH LI S LF
VIL       4    420   F YGG D C YLV   443   L H- W Q G AM-PAR M SSA P   479   MG K EP AH LM A IF
PVL       4    492   F YNQ S C YLV   515   L YY W Q G RFSSSE D KGA A   553   QN K EP NH FL E HF
SVL       4   1353   F HEG D A YVV  1391   Y FF W Q G RQSTVS E KGT S  1426   QG K EP PC FL Q CF
FLI       4    928   F YTQ D C YVF   984   V YF W Q G REASNM G WLT F  1023   QQ Q EN PK FL S HF
GRP125    4    361   F YSN K S YVC   385   I FF W E G LYSNQR N YIG Y   428   QN K EP QE FI N LF

PGS       5    545   L NSN D A FVL   559   A YL W V G TGASEA E KTG A   591   EG S EP DS FW E AL
DGS       5    587   L ASS D A FVL   603   I YI W N G LGASAF E KQA A   637   EG A EP DE FW E EL
XGS       5    224   L NSN D A FVL   238   S YL W V G QGSTNV E KNG A   270   EG Q ET DD FW G AL
VIL       5    539   L NSN D V FVL   553   C YL W Y E KGCSGD E REM G   586   EG Q EP PE FW V AL
PVL       5    617   L DSN D S FIL   633   S YI W V G KYSDEK E AAL Q   665   EG D ET SE FW E SL
SVL       5   1484   L RSR T S MVV  1500   I YL W H G CKAQAH T KEV G  1546   EG S EP LG FW D AL
FLI       5   1080   L NSE F C FIL  1101   V YA W V G RASDPD E AKL A  1136   EG E EP EN FF W VG
GRP125    5    479   L NSL D S FVF   494   I IV W H G KVSTEH Q REL A   530   QG K ES DN FW K II

PGS       6    650   L ATD D V MLL   664   V FV W V G KDSQEE E KTE A   706   QG F EP PS FV GW FL
DGS       6    694   L DSD D I MLL   708   I YL W V G YGVSEE E NGK L   751   QG K EP RV FK R MF
XGS       6    328   L ATD D V MLL   342   V YV W V G NEAQED E KKE A   384   QG F EP PT FI GW FL
VIL       6    643   L DEN D V MLL   657   I FF W I G KGANES E KEA A   699   QG F EP PT FT GW FM
PVL       6    726   L DSD D V MLL   740   I FV W V G KESSDT E KLM A   781   DG F HE FT FN FH
SVL       6   1619   A PQP A L FLV  1633   V YL W Q G WWPIEN K ITG S  1686   AG L EP LT FT NM FP
FLI       6   1190   L ADD D I MLL  1204   V YM W V G TQTSQV E IKL S  1247   KG N EQ HA FT RC FH
GRP125    6    628   L NSQ E C VLL   642   V FL W K G SKSTDQ K LND T   684   QY N ES PL FK SY FH
```

Figure 2B.

C

```
          (aa-no.)   PIP2-binding         F-actin-      F-actin- /
                                          severing      PIP2-binding

h-pgs     (132)   GYFKS..GLKYKKGGVASGF   KHVVPNEVVVQ   RLFQVKGRRV.VR
h-vil     (109)   GYFKQ..GLVIRKGGVASGM   KHVETNSYDVQ   RLLHVKGKRN.VV
d-pvl     (163)   SYFKSYGGPRYVAPLKLTSA   SAAIATAAKQY   KLFHLKGRRN.IR
GRP125    ( 50)   NLVSSSITLH..........   ........DDA   KLIQVTGKDEPFH
```

Figure 2C.

conserved amino acids important for segment tertiary structure (termed motif B, A, C; Way and Weeds, 1988) are found largely unchanged in GRP125 (Figure 2B). The repeat pattern of these characteristic motifs strongly suggests that GRP125 belongs to the family of gelsolin-like proteins.

When the sequence of GRP125 (Figure 2A) is compared with gelsolin, villin, and flightless I proteins or

the recently described supervillin (Kwiatkowski *et al.*, 1988a; Arpin *et al.*, 1988; Campbell *et al.*, 1993; Pestonjamasp *et al.*, 1997) (Figure 2B), the highest similarity is found for gelsolin. This observation is valid in comparisons made at the level of individual segments as well as the entire protein. On the other hand, from a sequence-based phylogenetic analysis it is clear that GRP125 is not a close relative of gelsolin. For example, human gelsolin/S2S3 and GRP125/S2S3 share an identity of 28%, which is significantly lower than the identity of 50% between the S2S3 regions of human gelsolin and villin (Kwiatkowski *et al.*, 1988a; Arpin *et al.*, 1988). However, this degree of sequence identity is in line with the identities of 24–31% calculated by comparing the S2S3 regions of gelsolin and villin with those of other more distantly related gelsolin family members, such as flightless I, protovillin, and supervillin.

Despite the apparent similarity of GRP125 to members of the gelsolin family, several relevant criteria distinguish it from other gelsolin-related proteins (Figure 1B). First, GRP125 only contains five gelsolin-like segments (Figures 1B, pointer a, and 2, A and B). This feature is unique among gelsolin-related proteins, which are usually built up of either three or six gelsolin domains. Several lines of evidence show that S1 is missing in GRP125, and that its first N-terminal segment corresponds to S2 in gelsolin proteins. For example, Van Troys *et al.* (1996) reported characteristic differences in the long helix of S1-type segments compared with the S2-type counterparts, which are responsible for the differential binding of G- or F-actin. The positively charged character of arginine or lysine residues at S2 positions, equivalent to gelsolin residues 211, 213, and 222, is absolutely conserved throughout S2 segments, whereas the corresponding helix positions in the S1 type are acidic or uncharged. In the first N-terminal segment of GRP125, lysine residues occur at those critical positions (GRP125 residues 113, 115, and 126) suggesting that this segment corresponds to an S2 domain. A comparison of sequences of single GRP125 segments with segments of gelsolin and its relatives clearly defines the organization of GRP125 segments as corresponding to the consecutive segments 2–6 of gelsolin (Figures 1B and 2, A and B).

Second, GRP125 lacks the conserved consensus sequences found at the interface between S1 and S2 in gelsolin related proteins (Figures 1B, pointer b, and 2C). Neither the region implicated in the severing activity of gelsolin-related proteins, nor the first phosphatidylinositol bisphosphate (PIP_2)-binding motif is present in GRP125. Critical amino acid residues of gelsolin involved in binding F-actin and the second phospholipid-binding site (Figure 2C, gelsolin residues 161–172) (Kwiatkowski *et al.*, 1989; Sun *et al.*, 1994) are only moderately conserved in GRP125.

Third, the N terminus of GRP125 harbors a unique 6-kDa N-terminal repetitive sequence of unknown function (Figure 1B, pointer a). Fourth, a prominent and unique feature of GRP125 is the presence of two highly repetitive, glutamate-rich stretches. The first stretch comprises of an almost homogeneous run of 25 glutamates and is located between segments 5 and 6 (Figure 1B, pointer c). The second glutamic acidic-rich region located after segment 6 contains 21 repeats of the motif EEV[I,T]K (Figure 1B, pointer d). Half of these repeats contain a third glutamate and form the variant EEEVK. Hypermixed charge runs (Karlin, 1995) involving glutamate and lysine residues occur in a range of proteins such as MAP1B (human MAP1B; Lien *et al.*, 1994), the neurofilament triplet proteins (e.g., human NFM; Myers *et al.*, 1987), or caldesmon (human caldesmon; Novy *et al.*, 1991). However, the almost invariant EEVK repeat includes a single noncharged (valine) residue in its middle, rendering this repeat a characteristic motif that is unique to GRP125. Sequence-based structure predictions (Lupas *et al.*, 1991; Lupas, 1996) suggest the glutamate-rich stretches together with their flanking regions have a very high probability of forming α-helical coiled-coil structures. Thus, selecting for apolar residues at positions *a* and *d* (weight × 2.5) the residues between 554–581 and 710–748 are calculated by MTIDK and MTK matrices to have a probability of >95% of forming a coiled coil (Figure 2A; matrices are derived from myosins, paramyosins, tropomyosins, intermediate filaments type I–V, desmosomal proteins, and kinesins [MTIDK], or from myosins, tropomyosins, and keratins [MTK]). Without using the weighting of apolar positions, the entire second glutamate-rich region of GRP125 is predicted to form a coiled-coil structure (Figure 2A). Fifth, a notable and unique attribute of GRP125 is a repetitive sequence module located at its very C terminus (Figure 1B, pointer e). This extension is ~20 kDa in size and does not reveal motifs or sequence patterns related to any annotated sequence structures.

GRP125 Localizes to Vesicular Compartments

Dot blots using recombinant polypeptide fragments (Gly-69–Phe-182, Glu-181–Ser-380, and Asn-379–Ile-878) show a strong and specific interaction of mAb 212-174-1 to a region between amino acids Gly-69 and Phe-182 of GRP125 (our unpublished results). However, this antibody proved to react poorly with the same polypeptide after SDS-PAGE and immunoblotting. To obtain antibodies suitable for both immunoblot and immunofluorescence analysis, polyclonal antibodies were raised against bacterially expressed fragments of GRP125 from *Dictyostelium*. The different GRP125 fragments used in immunizations used either segments 2 and 3 (GRP125/S2S3) or segment 3 and
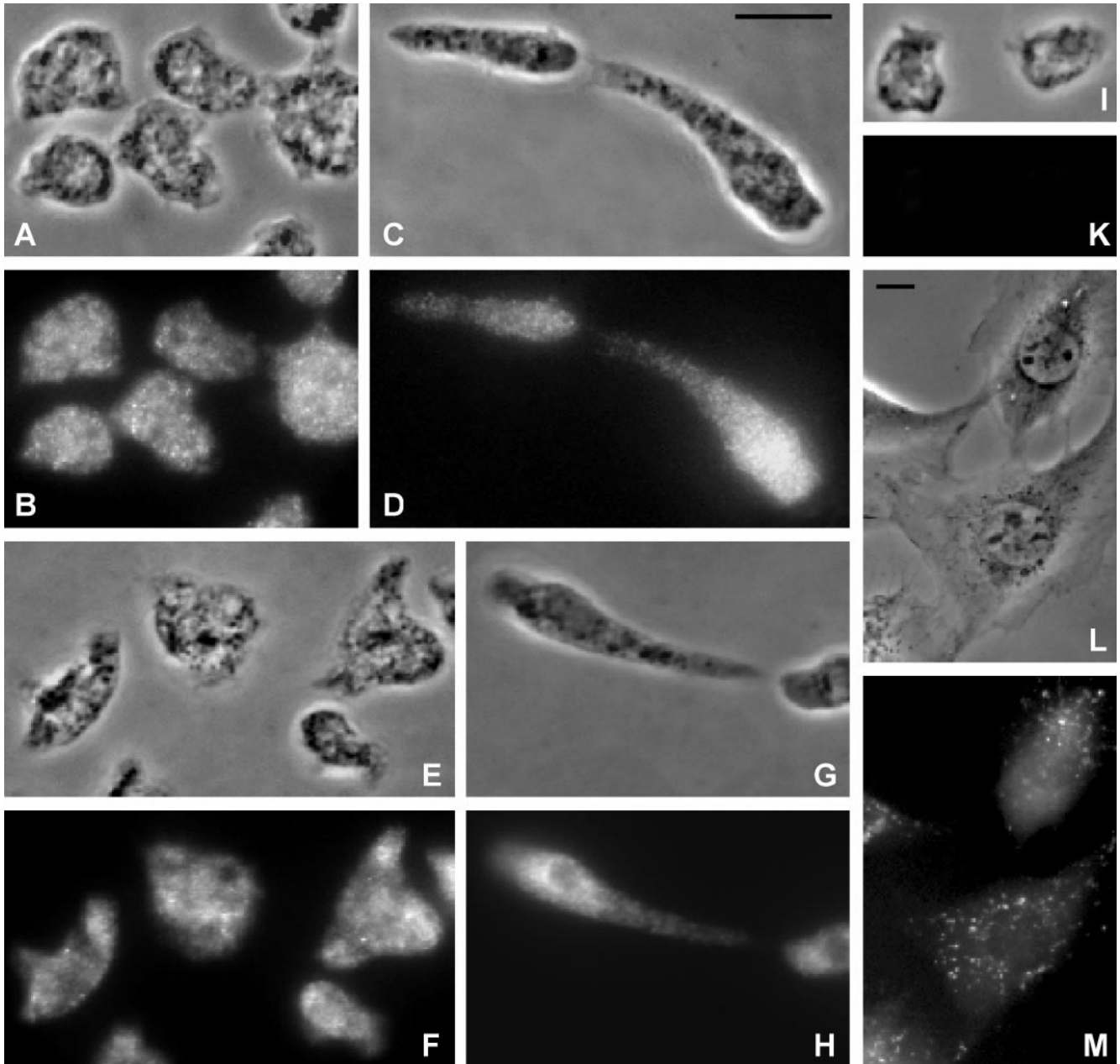
Figure 3. (A–K) GRP125 and its homologue localize to vesicular compartments in *Dictyostelium* cells. Corresponding phase-contrast micrographs (A, C, E, G, and I) and fluorescence images (B, D, F, H, and K) at different developmental stages are shown. Bar, 10 μm. (A–D) Localization of GRP125 in growth phase (A and B) and aggregation-competent (C and D) *D. discoideum* AX2 cells. Fixation was achieved using cold methanol; specimens were processed for indirect immunofluorescence labeling of GRP125 using the polyclonal anti-GRP125/S2S3 antibody followed by Cy3-labeled goat anti-rabbit IgG. (E–H) Immunofluorescence localization of both GRP125 and its homologue in growth phase (E and F) and aggregation-competent (G and H) *Dictyostelium* cells. Cells were fixed with picric acid/formaldehyde/70% ethanol. Labeling of both GRP125 and its homologue was performed using the polyclonal anti-GRP125/S3S4 antibody followed by the Cy3-labeled goat-anti rabbit IgG. (I and K) Background fluorescence using only the secondary Cy3 labeled goat-anti rabbit IgG antibody. (L and M) Incorporation of the recombinant rhodamine-labeled GRP125/S3S4 polypeptide to vesicle-like subcellular compartments after microinjection into living NIH/3T3 fibroblasts. (M) Fluorescence; (L) corresponding phase-contrast image. Bar, 10 μm.

most of segment 4 (GRP125/S3S4). The affinity-purified polyclonal rabbit anti-GRP125/S2S3 antibodies were shown to bind monospecifically to GRP125 (see below) and could be used to determine the subcellular distribution of GRP125 in vegetative and aggregating *Dictyostelium* cells.
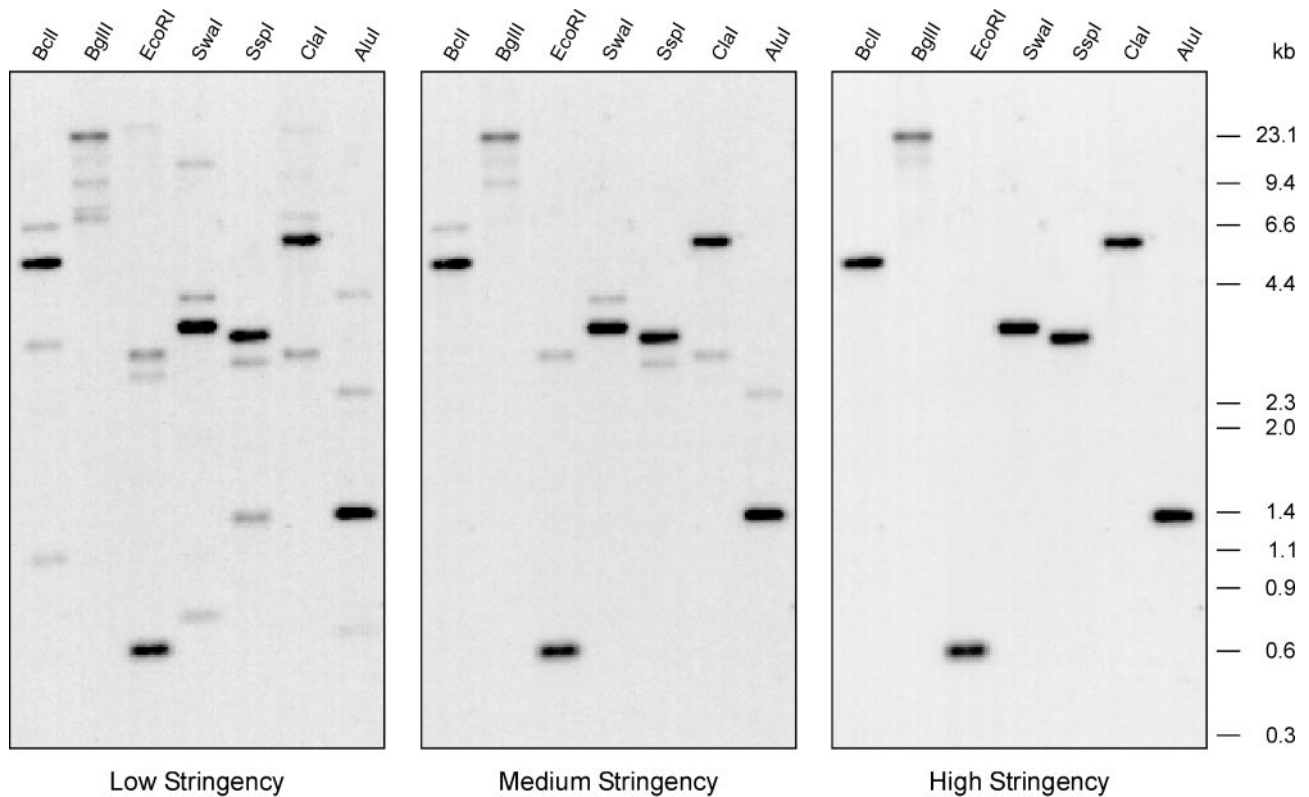
Figure 4. Southern blot analysis of the genomic organization of the GRP125-encoding gene indicates the presence of several closely related genes in *Dictyostelium*. Genomic DNA from *D. discoideum* AX2 was digested using the restriction endonucleases indicated, size fractionated by electrophoresis in agarose gels, and transferred to a Hybond-N membrane. The blot was hybridized under low-stringency conditions to a radioactively labeled cDNA probe of GRP125 (F2) and washed with low, medium, and high stringency.

Immunofluorescence labeling of growth phase cells revealed a pattern of numerous fluorescent punctae, which are dispersed throughout the cytoplasm (Figure 3, A and B). These punctae are heterogeneous in terms of their fluorescence intensity (Figure 3, A and B). The extensive intracellular distribution of the punctate GRP125 label, confirmed by confocal microscopy (our unpublished results), resembles the staining pattern of vesicular compartments in *Dictyostelium*; for example, it is related to the pattern of dispersed Golgi vesicles during cell division (Schneider *et al.*, 1998). These data suggest that GRP125 localizes to intracellular vesicles. Confocal microscopy showed that the fluorescent label was confined to those vesicular structures and not free in the cytoplasm (our unpublished results). GRP125 appeared to localize at the cytoplasmic outside of vesicles, which is supported by the observation that GRP125 is found predominantly in the soluble, cytoplasmic fraction. More than 70% of the cellular GRP125 pool sorts to the soluble fraction upon detergent-independent cell rupture in the absence of Ca^{2+} (our unpublished results).

Between 3 and 6 h after starvation, *Dictyostelium* cells rearrange their microfilament cytoskeleton and adopt a polarized morphology with a distinct leading front and trailing edge, and this state is associated with rapid chemotactic motility. Figure 3, C and D, shows that the localization of GRP125 in aggregation-competent *D. discoideum* cells is very similar to that observed in growth phase cells. Unlike other gelsolin-related proteins that perform a structural function, GRP125 does not accumulate at the cell cortex or at lamellipodia of motile cells (Brock and Pardee, 1988; Hofmann, 1994).

### Homologues of GRP125 Are Expressed in *D. discoideum*

In an effort to screen for other gelsolin-related proteins in *Dictyostelium*, Southern blot analysis was performed using the genomic region encoding segments 3 and 4 of GRP125 as a probe (probe F2). The single bands observed under conditions of high stringency suggest the presence of a single GRP125 gene in the *Dictyostelium* genome (Figure 4). However, under these lower-stringency conditions, three different, clearly visible bands were found (Figure 4, left). These cross-hybridizing fragments did not correspond to restriction

products of the well-characterized gelsolin-related genes in *Dictyostelium*, severin, and protovillin because of the different fragment sizes observed in Southern blot analysis (our unpublished results). For example, the *Eco*RI digest produced cross-hybridizing fragments of 2.6, 2.9, and ~20 kb, which differed from the 3.8-kb fragment obtained from the severin gene (André *et al.*, 1988) and the 6.6- and 11-kb fragments from the protovillin gene (Hofmann *et al.*, 1993). One of these three genes appeared to be very similar to the GRP125 gene, because its cross-hybridization to the probe persisted even under conditions corresponding to medium stringency (Figure 4).

Immunoblots of total protein extracts of *D. discoideum* were probed using the polyclonal anti-GRP125/S3S4 antibody. Whereas the polyclonal anti-GRP125/S2S3 antibody specifically recognized GRP125, the polyclonal anti-GRP125/S3S4 antibody strongly bound to a second protein of slightly higher electrophoretic mobility (Figure 5A). The second protein band labeled by the anti-GRP125/S3S4 antibody does not correspond to a proteolytic breakdown product of GRP125, as revealed by a distinct regulation and the unaltered expression of this protein in the GRP125-null background (see below). The apparent molecular masses measured by SDS-PAGE analysis were 142 kDa for GRP125 and 134 kDa for the second, related protein. The following data also suggest that GRP125 and the 134 kDa protein are homologous proteins: 1) the strength and specificity of the reaction of the affinity-purified anti-GRP125/S3S4 antibody against the 134 kDa protein; 2) their similar apparent molecular mass; and 3) their similar pI of ~4.6 (our unpublished results), which indicates a matching amino acid distribution. The close similarity between GRP125 and the 134-kDa protein supports our claim that the 134-kDa polypeptide is produced by the gene that was found to be highly similar to the GRP125 encoding gene in Southern blot analysis (see above; Figure 4; medium stringency). The difference between the values calculated (124.8 kDa) and measured (142 kDa) for GRP125 probably reflects a retarded mobility of GRP125 caused by local hypercharges in its glutamate-rich stretches. For example, lobster gelsolin has a high acidic content and migrates with an apparent molecular mass 22 kDa larger than calculated (105 vs. 83 kDa; Lück *et al.*, 1995).

The distribution of GRP125 and its homologue was compared by immunofluorescence analysis using a variety of fixation protocols (Figure 3). From a series of immunofluorescence experiments an identical vesicle-like staining was observed for the anti-GRP125/S3S4 antibody (Figure 3, E–H), which recognized both homologous proteins and the GRP125-specific anti-GRP125/S2S3 antibody (Figure 3, A–D). These data suggest that both molecules localize to the same structures. Control
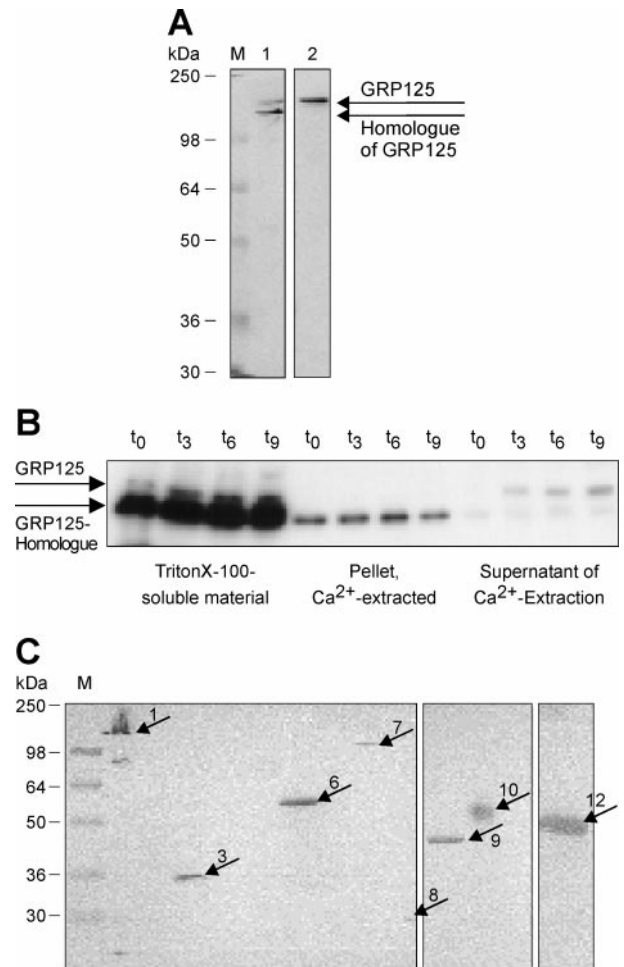
Figure 5. (A) GRP125 from *Dictyostelium* and its closely related homologue. Western blot analysis of a lysate from vegetative *D. discoideum* cells using (1) the polyclonal anti-rabbit *Dictyostelium* GRP125/S3S4 antibody or (2) the polyclonal anti-rabbit *Dictyostelium* GRP125/S2S3 antibody. M, molecular weight marker. The anti-GRP125/S2S3 antibody monospecifically binds GRP125; the anti-GRP125/S3S4 antibody recognizes a second 125-kDa gelsolin-related protein. (B) Localization of GRP125 and its homologue to Triton X-100–soluble and –insoluble cellular fractions of *Dictyostelium* and extractability upon Ca^{2+} treatment. Western blot analysis of subcellular fractions from *D. discoideum* after starvation in suspension using the anti-GRP125/S3S4 antibody. Shown are relative amounts of GRP125 and its homologue present in the Triton X-100–soluble cellular material, the Triton X-100–insoluble material extracted by Ca^{2+}, and the detergent- and Ca^{2+}-insoluble material. The fraction of GRP125 present in the Triton X-100–insoluble material is completely extracted by addition of Ca^{2+}; the GRP125 homologue is not solubilized by Ca^{2+}. (C) Presence of GRP125-related proteins in cells from lower to higher eukaryotes. Western blot analysis of cell extracts from different sources using the anti-GRP125/S3S4 antibody. M, molecular weight marker. Next to 1 (*D. discoideum* AX2 [control]), cell lysates were tested from *Saccharomyces cerevisiae* (2), *S. pombe* (3), human hepatocytes (4), Cv-1 cells (5), SF9 cells (6), mouse brain tissue (7), macrophages (8), muscle tissue of mouse (9), rat (10), and human (11), and NIH/3T3 fibroblasts (12). The polyclonal antibody reacted specifically with distinct proteins of differing sizes in a range of cell types. Prominent bands marked in the lysates are highlighted by arrows; arrow numbers code for the cell source.
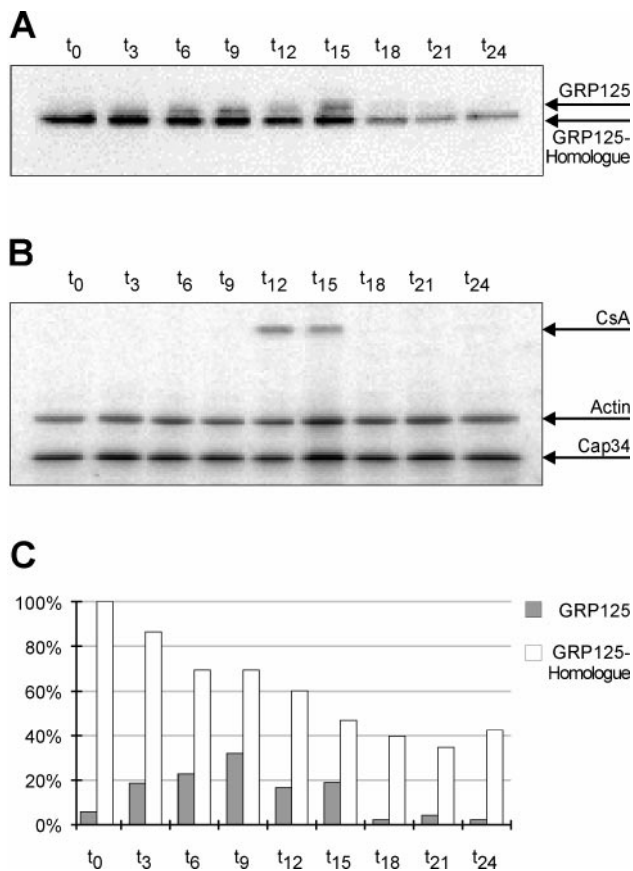
Figure 6. (A) Expression of GRP125 and its homologue is developmentally regulated. Samples of filter-developed *D. discoideum* AX2 cells were taken at indicated time points, and 20 μg of each lysate were analyzed by Western blotting using the rabbit anti-GRP125/S3S4 antibody (exposed to BioMax x-ray film; for a quantification see C). (B) Equal loading was confirmed by monitoring the approximately constant expression of actin and Cap34. Correct developmental progression was validated by the characteristic expression pattern of the CsA protein during development, the major adhesion protein involved in the EDTA-stable cohesion of aggregating cells (Müller and Gerisch, 1987). (C) Quantification using the Phosphoimager. The signal of the GRP125 homologue in growth phase cells is arbitrarily set to 100%; loading differences were accounted for by taking values relative to Cap34 signals. Expression of GRP125 increases by an order of magnitude until t_{12} (aggregation) and drops after t_{15} (pseudoplasmodial stage). The homologue declines continually to ~50% at t_{24} (culmination starts at t_{18}).

experiments using only the secondary antibody showed no staining above background level (Figure 3, I and K).

Expression of GRP125 Is Developmentally Regulated

The expression of GRP125 during the developmental cycle of *D. discoideum* was examined using filter-developed cells (Figure 6, A–C). GRP125 is present in vegetative cells in minor quantities. The transition from growth phase (t_0) to early aggregation phase (t_9)

led to an increase in the level of GRP125 by almost one order of magnitude (Figure 6C). The maximal GRP125 protein level in aggregation phase cells (t_9) is approximately maintained until the slug stage (t_{15}). Thereafter the GRP125 level rapidly decreased to barely detectable amounts during culmination and fruiting body formation. Evidently, expression of GRP125 is tightly regulated during development. Because GRP125 mRNA levels likewise increase by an order of magnitude at the onset of starvation (our unpublished results), the expression of GRP125 appears to be transcriptionally regulated. The expression profile of the GRP125 homologue differed markedly from that of GRP125, because the homologue was maximally expressed in vegetative cells. The GRP125 homologue protein level gradually declined during development to an amount in fruiting bodies (t_{24}) that equaled 50% of the protein in growth phase cells (Figure 6C).

Partitioning of GRP125 in Triton X-100–soluble and –insoluble Cellular Fractions

The distribution of GRP125 and its homologue in Triton X-100–soluble and –insoluble cellular fractions was analyzed by Western blotting using the anti-GRP125/S3S4 antibody, which recognizes both GRP125 and the GRP125 homologue (Figure 5B). The majority of GRP125 was present in the Triton X-100–soluble fraction at all stages of development, a feature that GRP125 shares with its homologue and other proteins such as DdPlastin, α-actinin, DdLIM, GFP-DdLIM, and tyrosine-phosphorylated actin (Jungbluth, 1996; Marriott and Stocker, unpublished results). However, a minor amount of GRP125 was found in the Triton X-100–insoluble cellular material and was extracted quantitatively on addition of Ca^{2+} to the Triton X-100–insoluble material. In contrast, the small amount of the GRP125 homologue in the insoluble fraction was not eluted by Ca^{2+} (Figure 5B). Our data show that the majority of GRP125 is removed from the cells by detergent treatment. The association of the remaining population of GRP125 with the Triton X-100–insoluble fraction is probably regulated by Ca^{2+}, either through direct binding of Ca^{2+} by GRP125 or through an interaction with a Ca^{2+}-regulated protein.

Inactivation of the GRP125 Gene

To understand the in vivo function of GRP125 and its role in development, we prepared mutant cell lines lacking GRP125. The construct used for transfection of *D. discoideum* AX2 replaced the genomic region coding for residues Glu-181 to Ser-380 of GRP125 with the blasticidin S resistance cassette (Bsr cassette; Sutoh, 1993; Figure 7A). This approach was designed to irreversibly inactivate the GRP125-gene via homologous recombination. After transformation, blasticidin S–re-

sistant clones were tested for the absence of GRP125 in immunoblot analysis using the anti-GRP125/S3S4 antibody. Three independent GRP125-deficient mutants, GRP125⁻/17, GRP125⁻/18, and GRP125⁻/C, failed to express GRP125 (Figure 7B) and were chosen for further characterization. Using an *Eco*RI–*Bgl*II digest, Southern blots of AX2 and mutants were analyzed with the F1 probe that hybridized to a 2.8-kb fragment of AX2 DNA (Figure 7C). At the DNA level the labeled fragment of GRP125 mutants showed a shift up to 3.8 kb (Figure 7C). This increase reflected the loss of the second *Eco*RI site in the replacement construct, which added to the genomic 3' *Eco*RI fragment a 1-kb part of the Bsr cassette. A hybridization experiment using the Bsr coding region as a probe labeled the same bands as the GRP125-specific probe and proved the integration of the construct into the GRP125 gene. Solitary bands in Southern blot analysis demonstrated single insertions of the construct into the GRP125 gene for mutants GRP125⁻/18 and GRP125⁻/C. An additional band in the restricted GRP125⁻/17 DNA indicated another, random insertion of the construct into the *Dictyostelium* genome; however, all three mutants were indistinguishable in respect to their phenotypical characteristics.

Growth of GRP125⁻ Cells and Progression through the Developmental Cycle

Growth of *Dictyostelium* mutants on lawns of bacteria or axenically in shaken suspension is a complex process that requires a number of cellular functions such as cell division, phagocytosis, adhesion, locomotion, pinocytosis, and tolerance against shearing stress. To assess growth characteristics of GRP125⁻ cells, AX2 and mutant cells were inoculated on a lawn of *E. coli* B/2, and the increase in colony diameter was taken as a relative measure of the growth rate (Figure 8A). GRP125⁻-colonies had growth rates that correlated with those measured for AX2 cells. Furthermore, axenically grown GRP125⁻ cells were indistinguishable from AX2 cells with respect to generation times and maximal cell densities (Figure 8B). These data suggest that the cellular functions described above appear in-

Figure 7. (A) Schematic presentation of the replacement strategy yielding the inactivation of the GRP125 gene in *Dictyostelium*. The 1.8-kb genomic region at the 5' end of the GRP125 gene was amplified via PCR (small arrows) and cloned into pGEM-5Z. The *Eco*RI–*Eco*RI-fragment (light gray) was deleted (flash in light gray) (1) and replaced by blunt-end insertion of the Bsr resistance cassette (2), Act15P, actin 15 promotor; Act8T, actin 8 terminator; Bsr, blastici-din-S deaminase gene. Restriction sites marked in gray got lost (cross) or introduced in the replacement construct. A kilobase ruler refers to nucleotide positions in the GRP125 gene (A of ATG = 1). (B) Western blot analysis of homogenates of three independent GRP125-deficient mutants (GRP125⁻/17, GRP125⁻/18, and GRP125⁻/C)

Figure 7 (cont.). and AX2 cells. Cell lysates (1 × 10⁶ cells, growth phase) were analyzed with the polyclonal anti-GRP125/S3S4 antibody. GRP125⁻/17, GRP125⁻/18, and GRP125⁻/C fail to express GRP125 but produce the GRP125 homologue. (C) Comparative Southern blot analysis of genomic DNA of GRP125-deficient cells (GRP125⁻/17 [1], GRP125⁻/18 [2], and GRP125⁻/C [3]) and AX2 cells (4). Genomic DNA from *D. discoideum* AX2 and the mutants was *Eco*RI–*Bgl*II double digested, size fractionated by electrophoresis in agarose gels, and transferred to a Hybond-N membrane. The blot was hybridized to radio-actively labeled DNA probes of GRP125 corresponding to a fragment exactly 3' of the deleted *Eco*RI–*Eco*RI fragment (GRP125-specific probe F1, bp 1228–2727 of the GRP125 coding region) or the Bsr encoding sequence.
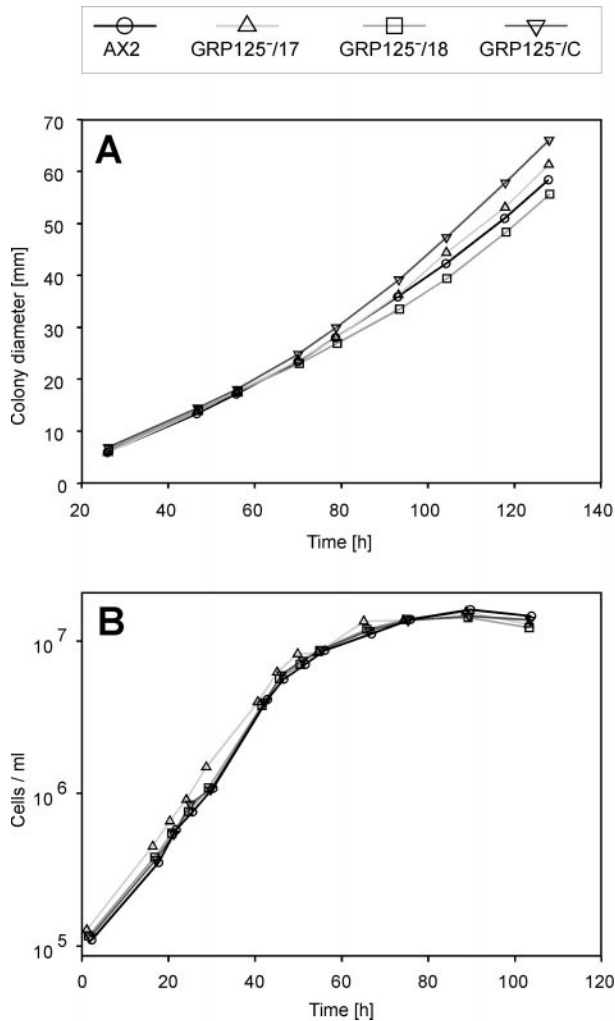
Figure 8. Growth of GRP125-deficient cells (GRP125⁻/17, GRP125⁻/18, and GRP125⁻/C) in comparison with AX2. Evaluations were averaged from (A) five growth experiments on a lawn of *E. coli* B/2 at 21°C (A) and four growth experiments in suspension (21°C) using axenic medium after inoculation with 5×10^4 cells (B). Growth is not impaired by deficiency of GRP125.

tact in vegetative GRP125-deficient cells. GRP125⁻ cells are able to complete the developmental cycle and passed through all stages of development without macroscopically evident disorders (compare developmental stages of GRP125⁻ and AX2 cells depicted in Figure 9C). Mutant cells develop a regular feeding fringe; they are able to form aggregates, slugs, and morphologically normal fruiting bodies with functional spores. The timing of progression through development is not altered by GRP125 deficiency.

The Pseudoplasmodium Stage of GRP125⁻ Mutants Exhibits a Defect in Phototactic Orientation

The expression profile of GRP125 during development suggests it exerts its function late during ag-

gregation or in the slug (compare Figure 6). In the natural habitat of *D. discoideum*, an important survival task for the slug is to migrate to the soil surface to ensure its progeny will be dispersed to more favorable environments. The orientation of slugs toward a light source is a critical prerequisite for this function (reviewed in Fisher, 1997). The ability of slugs of the GRP125-deficient mutant to perform a phototactic response was analyzed in a phototaxis assay (Wallraff, 1997). Figure 9A shows the migration paths of GRP125⁻ slugs compared with AX2 slugs. "Wild-type" AX2 slugs approached the light source starting from their point of application in a straightforward manner, whereas the mutant slugs had severe problems in their orientation. Initially, the mutant slugs moved in the right direction, although they often made slight detours during this maneuver. However, shortly after this first phase, GRP125-deficient slugs appeared to lose complete control of their direction, most likely because they failed to readjust their "homing" and progressively acquired a random walk behavior. After 3 d in the chamber, GRP125⁻ slugs were found at random locations with respect to the light source. In most cases they made repeated turns in this final phase and crawled in small circles. Circle paths were also found with wild-type AX2 slugs after 3 d of random walk in complete darkness. An evaluation of 109 trails (≥1 cm) of GRP125⁻ slugs did not produce a single successful approach toward the light source. Most of the GRP125⁻ mutant slugs sporulated immediately at the point of application on the plate, and in most cases less than four trails were observed per plate. This corresponded to only a third of the number of trails that AX2 slugs formed in this experimental setup. GRP125 might therefore also be involved in the signal pathway that controls a slug's decision to start migration or culminate immediately (Schindler and Sussman, 1977; Williams *et al.*, 1984).

Significantly, GRP125⁻ slugs were not impaired in their ability to migrate over the agar plate. Control experiments without light revealed no difference of the random walk behavior of GRP125⁻ slugs compared with AX2 slugs (Figure 9B). GRP125⁻ slugs were able to migrate for long distances in darkness, and similar numbers of trails were observed for AX2 and GRP125⁻. The evident defect of GRP125⁻ slugs in the phototaxis assay is therefore a true phototaxis defect. To further investigate the phototaxis defect, fruiting bodies of mutant cells were analyzed for their photodetection and orientation toward a light source. As seen in Figure 9C, GRP125-deficient fruiting bodies were able to sense the direction of incident light, and they turned toward the light source just as well as the fruiting bodies of AX2 cells.
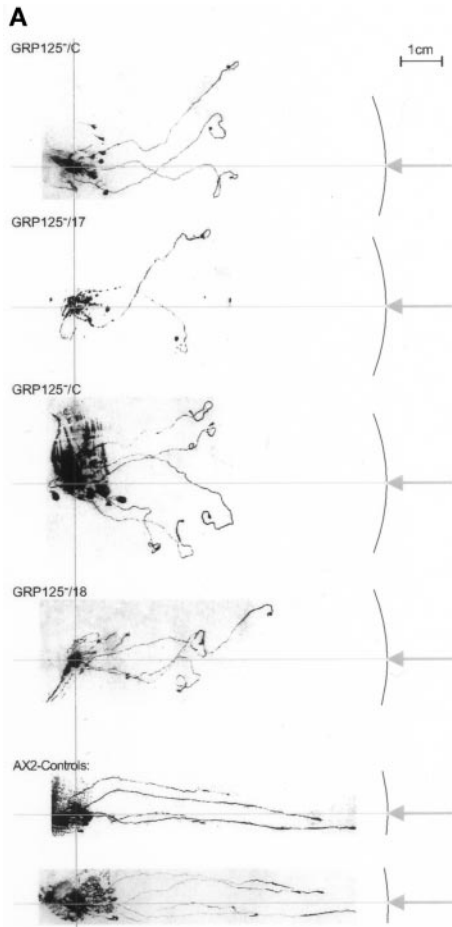
Figure 9. (A) Phototactic behavior of GRP125-deficient slugs (GRP125⁻/17, GRP125⁻/18, and GRP125⁻/C) in comparison with AX2 slugs. Cells (1×10^7) were incubated for 3 d in a phototaxis chamber. Subsequently, trails and cell material were blotted and stained with Coomassie Blue. The light hole and light path in the chamber are represented by the arrow and horizontal line; the outline of the phototaxis chamber is indicated as well. Points of cell application, apparent from the mass of spore material formed, are aligned, illustrated by the vertical line in light gray. AX2 slugs directly approach the light hole along the light path; slugs of mutants deviate shortly after the start of migration and progressively lose orientation. (B) Migration in complete darkness of GRP125-deficient slugs in comparison with AX2 slugs. Cells (1×10^7) were incubated for 3 d in complete darkness in the phototaxis chamber and processed as in A. The capacity for long-range migration is not altered by GRP125 deficiency. (C) Photodetection of GRP125-deficient and AX2 fruiting bodies. A lawn of *E. coli* B/2 was point inoculated, incubated for 4 d in the phototaxis chamber, and photographed. Consecutive frames in the top row (1–3) show experiments using AX2, and those in the lower row (4–6) show GRP125⁻. Arrows indicate the position of the light hole. Bar, 1 cm. Fruiting bodies turned to the direction of the light source in the presence and absence of GRP125.
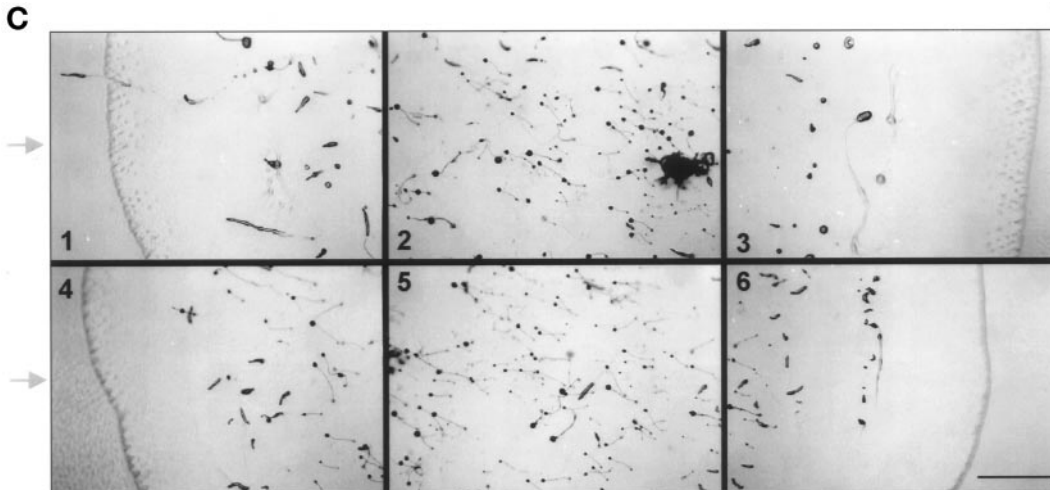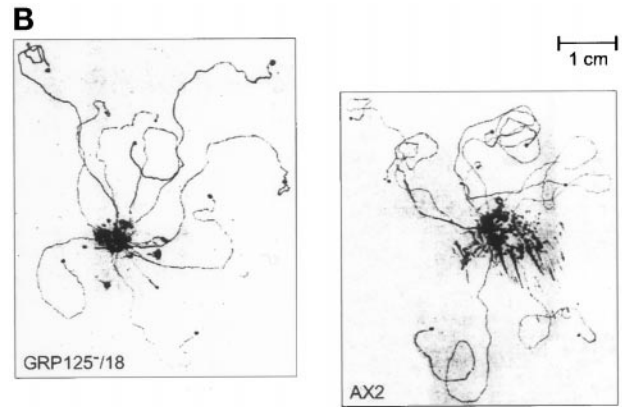
Figure 9.

Further Representatives of the GRP125 Type in Cells from Different Sources, Ranging from Lower to Higher Eukaryotes

Western blot analysis was performed on homogenates of cells from different sources using the affinity-purified polyclonal anti-GRP125/S3S4 antibody (Figure 5C). This antibody specifically labeled distinct protein bands with different molecular masses in lysates of *Schizosaccharomyces pombe*, SF9 cells, mouse brain tissue, macrophages, mouse and rat muscle tissue, and of NIH/3T3 fibroblasts. Because the antibody was directed against gelsolin-like segments 3 and 4 of GRP125, these proteins should belong to the gelsolin family of actin-binding proteins. Most of the proteins detected in the immunoblot shown in Figure 5C could not be attributed to sizes of known gelsolin-related proteins, and furthermore, the antibody did not recognize bona fide gelsolin-related proteins present in these lysates. For example, the anti-GRP125/S3S4 antibody did not recognize the 82-kDa gelsolin in mammalian cell lysates. Similarly the antibody did not cross-react with the 38-kDa CapG in the NIH/3T3 fibroblast lysate or with the gelsolin-like proteins severin (40 kDa) or protovillin (109 kDa) in the *Dictyostelium* lysate.

Immunofluorescence analysis of NIH/3T3 fibroblasts or human kidney cells (293 cells; our unpublished results) using the anti-GRP125/S3S4 antibody exhibited a similar punctate labeling pattern as was observed in *Dictyostelium* cells. A similar distribution was found by microinjection of the polypeptide spanning residues Asp-60 to Leu-308 of GRP125 (corresponding to S2 and S3) into NIH/3T3 fibroblasts. This peptide was found to be specifically incorporated into vesicle-like structures that were previously observed in the immunofluorescence analysis (Figure 3, L and M). The punctate label of GRP125 in *Dictyostelium* parallels that of supervillin in Madin–Darby bovine kidney cells (Pestonjamasp *et al.*, 1997); however, the proteins reveal different distributions. The identical localization of a rhodamine-labeled GRP125/S2S3 peptide to vesicular compartments in mouse fibroblasts suggests the homologous proteins in mouse and *Dictyostelium* might share a related function.

DISCUSSION

Gelsolin, severin, and several of their relatives control microfilament length, number, and availability of barbed ends on actin filaments for polymerization (Weeds and Maciver, 1993; Eddy *et al.*, 1997; Han *et al.*, 1997). These proteins are generally active at cellular sites that continually require dynamic regulation of actin filament length, such as lamellipodia and the cell cortex. The difference in the subcellular distribution of GRP125 in *D. discoideum* compared with other gelso-lin-like proteins suggests it is not involved in the protrusion of filopodia or lamellipodia or the organization of cell shape. Rather, the localization of GRP125 to structures that appear punctate in the immunofluorescence experiments suggests a role more related to the structure or function of intracellular vesicles.

We have argued on the basis of significant sequence similarity and critical differences of GRP125 to members of the gelsolin family of actin-binding proteins that GRP125 represents a new type of a gelsolin-related protein. Fundamental differences in the microfilament-directed activities of GRP125 compared with other gelsolin-related proteins are anticipated by analyses of their primary structures. Gelsolin-like proteins contain six different segments schematized in Figure 1A. The S1 domain is completely absent in GRP125, and furthermore, significant deviations from consensus sequences exist in the S1S2 linker region and in the first part of S2. According to models of gelsolin domain structure–activity relationships, these deletions should result in a loss of several gelsolin-related protein functions: high-affinity capping of actin filaments depends on activities that reside in S1 (Weber *et al.*, 1991; McLaughlin *et al.*, 1993), whereas an efficient severing activity also requires sites at the beginning of S2 (Kwiatkowski *et al.*, 1985; Way *et al.*, 1989; McGough *et al.*, 1998). Critical differences in the S2 domain would also suggest that GRP125 lacks actin nucleation activity. A corresponding stretch deleted in the S2 segment of protovillin is considered responsible for the inability of protovillin to nucleate filaments (Hofmann, 1994).

Similar to GRP125 in *D. discoideum*, gelsolin in mammalian cells is solubilized to a large extent by treatment with Triton X-100 under Ca^{2+}-free conditions at neutral pH (platelets [Barkalow *et al.*, 1996], nonadherent neutrophils [Wang *et al.*, 1997], myoblasts [Scholz and Hinssen, 1995], and polymorphonuclear leukocytes [Watts *et al.*, 1995]). However, in *Dictyostelium* Ca^{2+} treatment coelutes GRP125 along with a specific set of microfilament proteins from the Triton X-100–insoluble fraction (Jungbluth *et al.*, 1995; Prassler *et al.*, 1997, 1998), suggesting that GRP125 associates with the actin cytoskeleton. Actin is known to be involved in anchoring and transport of vesicles (Kuznetsov *et al.*, 1992; Muallem *et al.*, 1995; van Deurs *et al.*, 1995). Defaque *et al.* demonstrated a crucial role of the actin-binding protein ezrin and phosphoinositides for actin nucleation on phagosomal membranes (Defacque, Habermann, Egeberg, Diakonova, Roy, Mangeat, Voelter, Marriott, Pfannstiel, Faulstich, and Griffiths, unpublished data), and other actin-binding proteins are known to associate directly or indirectly with actin on the surface of the phagosome (Desjardins *et al.*, 1994). Based on data presented herein, it is not unreasonable to speculate that GRP125 acts, directly or in-

directly, at the interface of actin and intracellular vesicles.

Experiments with bacterially expressed GRP125 fragments did not reveal direct binding of GRP125 segments 2 and 4 to F- or G-actin (our unpublished results), as has been observed for other gelsolin relatives (Way *et al.*, 1989; Eichinger and Schleicher, 1992; Pope *et al.*, 1995). These data do not necessarily rule out a microfilament association of GRP125, because it might involve both GRP125's gelsolin core and its additional N- and C-terminal domains that constitute approximately half of GRP125's residues. The long actin-binding helix of S2 is conserved in GRP125, whereas the C-terminus of GRP125 reveals basic patches that might resemble potential cryptic actin-binding sites (e.g., KDKRK and KKNKNKNKKKHNR). Furthermore, because the function of GRP125 apparently does not involve modulation of actin filament dynamics, a direct interaction with actin itself is not obligatory. One or more actin-binding proteins could mediate the association of GRP125 with the actin cytoskeleton, for example, through its presumptive coiled-coil regions (Lupas, 1996). Interestingly, the computed coiled-coil region originating in the poly-glutamate run of GRP125 represents an extension on the exposed S5S6 linker described in horse plasma gelsolin (Burtnick *et al.*, 1997). Our sequence analysis predicted that the EEVK repeats are evidently not required to stabilize coiled-coil formation, and these repeat motifs may be involved in the recognition of a target protein.

A search for genes or gene products related to GRP125 using DNA and protein probes directed against segments 3 and 4 of GRP125 failed to label known members of the gelsolin family, such as gelsolin, capG, adseverin, severin, and protovillin. On the other hand, several proteins were specifically detected in *Dictyostelium* samples or heterologous homogenates of lower and higher eukaryotes. We therefore suggest that these putative gelsolin-like genes and their products show a closer similarity to GRP125 than to prototypical gelsolin. The different molecular weight of the proteins detected by the anti-GRP125/S3S4 antibody is of particular interest, because recent publications have described gelsolin-related proteins with unusual segment organizations. Twinfilin from yeast exhibits two cofilin-like domains (Van Troys *et al.*, 1997; Goode *et al.*, 1998), and murine adseverin (D5) misses the fifth gelsolin segment (Robbens *et al.*, 1998). Gelsolin-related proteins of the GRP125 type are well represented in the *D. discoideum* genome, because in addition to a GRP125 homologue at least two other GRP125-like proteins were identified by Southern blot analysis. Although GRP125 and its homologue share similar molecular masses, pIs, and subcellular localization, they have distinct expression patterns during development, and the gene products differ in their Ca^{2+}-dependent association with the Triton X-100–insoluble cellular fraction.

In *Dictyostelium*, different stages during development require particular activities of the actin cytoskeleton, which are governed by expression of specific actin-binding proteins. Within 6 h of starvation, individual cells become polarized and highly motile, whereas at 12–16 h a tissue-like pseudoplasmodium must achieve the concerted movement of its ~100,000 cells in its search for light and a favorable temperature (reviewed by Gerisch, 1987; Fisher, 1997; Fisher *et al.*, 1997). GRP125 is barely present in vegetative cells, and accordingly, GRP125-deficient cells grow normally. In general, GRP125-null cells were only marginally perturbed during most of the different developmental stages. However, a clear-cut primary defect of the knock-out mutant was observed at the multicellular pseudoplasmodial stage. Lack of GRP125 causes a progressive degeneration of the ability of slugs to readjust their orientation toward the light. The initial phototactic reaction of GRP125-null slugs suggests that GRP125 itself is not responsible for the detection of light. This is confirmed by the fact that GRP125-deficient fruiting bodies are able to detect light and to respond by turning toward the source. Thus, the orientation toward a light source may be another instance of similar signaling pathways operating in slugs and fruiting bodies (Bonner *et al.*, 1985, 1988; Feit *et al.*, 1987). Because the same type of cells, the (pre)stalk cells, control photodetection and phototactic behavior, identical components and mechanisms appear to be engaged for light detection both in slugs (Fisher, 1997) and in fruiting bodies, and evidently this process is not affected in fruiting bodies lacking GRP125. Moreover, GRP125-null slugs are perfectly able to migrate without GRP125. Apparently, it is the sustained readjustment of the orientation to light that is impaired in the absence of GRP125. We have argued that features of its primary structure predispose GRP125 to having an adapter function (see above), and this might couple photodetection to the locomotory apparatus of cells in the slug. In this context it is interesting that the association of a fraction of GRP125 with the Triton X-100–insoluble cellular material is determined by the presence of Ca^{2+}, which is a central signal transduction component in phototaxis (Fisher, 1997).

Both the molecular and the functional characterization introduce GRP125 as a new type of a gelsolin-related molecule. This new type of a gelsolin-related molecule may be involved in providing a functional connection between intracellular vesicles and the microfilament cytoskeleton. GRP125 is evidently indispensable during phototactic migration of *Dictyostelium* pseudoplasmodia: in the natural habitat of *D. discoideum*, GRP125-deficient slugs would most often fail to approach the soil surface. Without access to the surface, fruiting bodies produced in the course of development would not be able to disperse their spores to

locations with a sufficient supply of bacteria. We conclude therefore that GRP125 is essential for propagation and thus viability of *Dictyostelium* cells.

ACKNOWLEDGMENTS

REFERENCES

Altschul, S.F., Madden, T.L., Schäffer, A.A., Zhang, J., Zhang, Z., Miller, W., and Lipman, D.J. (1997). Gapped BLAST and PSI-BLAST: a new generation of protein database search programs. Nucleic Acids Res. *25*, 3389–3402.

Ampe, C., and Vandekerckhove, J. (1987). The F-actin capping proteins of *Physarum polycephalum*: cap42(a) is very similar, if not identical, to fragmin and is structurally and functionally very homologous to gelsolin; cap42(b) is *Physarum* actin. EMBO J. *6*, 4149–4157.

André, E., Lottspeich, F., Schleicher, M., and Noegel, A.A. (1988). Severin, gelsolin, and villin share a homologous sequence in regions presumed to contain F-actin severing domains. J. Biol. Chem. *263*, 722–727.

Ankenbauer, T., Kleinschmidt, J.A., Walsh, M.J., Weiner, O.H., and Franke, W.W. (1989). Identification of a widespread nuclear actin-binding protein. Nature *342*, 822–825.

Arpin, M., Pringault, E., Finidori, J., Garcia, A., Jeltsch, J.-M., Vandekerckhove, J., and Louvard, D. (1988). Sequence of human villin: a large duplicated domain homologous with other actin-severing proteins and a unique small carboxy-terminal domain related to villin specificity. J. Cell Biol. *107*, 1759–1766.

Barkalow, K., Witke, W., Kwiatkowski, D.J., and Hartwig, J.H. (1996). Coordinated regulation of platelet actin filament barbed ends by gelsolin and capping protein. J. Cell Biol. *134*, 389–399.

Bazari, W.L., Matsudaira, P., Wallek, M., Smeal, T., Jakes, R., and Ahmed, Y. (1988). Villin sequence and peptide map identify six homologous domains. Proc. Natl. Acad. Sci. USA *85*, 4986–4990.

Bertholdt, G., Stadler, J., Bozzaro, S., Fichtner, B., and Gerisch, G. (1985). Carbohydrate and other epitopes of the contact site A glycoprotein of *Dictyostelium discoideum* as characterized by monoclonal antibodies. Cell Differ. *16*, 187–202.

Bonner, J.T., Chiang, A., Lee, J., and Suthers, H.B. (1988). The possible role of ammonia in phototaxis of migrating slugs of *Dictyostelium discoideum*. Proc. Natl. Acad. Sci. USA *85*, 3885–3887.

Bonner, J.T., Hay, A., John, D.G., and Suthers, H.B. (1985). pH affects fruiting and slug orientation in *Dictyostelium discoideum*. J. Embryol. Exp. Morphol. *87*, 207–214.

Bradford, M.M. (1976). A rapid and sensitive method for the quantitation of microgram quantities of protein utilizing the principle of protein dye-binding. Anal. Biochem. *72*, 248–254.

Bretscher, A., and Weber, K. (1980). Villin is a major protein of the microvillus cytoskeleton which binds both G and F actin in a calcium-dependent manner. Cell *20*, 839–847.

Brock A.M., and Pardee J.D. (1988). Cytoimmunofluorescent localization of severin in *Dictyostelium* amoebae. Dev. Biol. *128*, 30–39.

Brundage, R.A., Fogarty, K.E., Tuft, R.A., and Fay, F.S. (1993). Chemotaxis of newt eosinophiles: calcium regulation of the chemotactic response. Am. J. Physiol. *265*, 1527–1543.

Burtnick, L.D., Koepf, E.K., Grimes, J., Jones, E.Y., Stuart, D.I., McLaughlin, P.J., and Robinson, R.C. (1997). The crystal structure of horse plasma gelsolin: implications for actin severing, capping, and nucleation. Cell *90*, 661–670.

Campbell, H.D., Schimansky, T., Claudianos, C., Ozsarac, N., Kasprzak, A.B., Cotsell, J.N., Young, I.G., deCouet, H.G., and Miklos G.L.G. (1993). The *Drosophila melanogaster* flightless I gene involved in gastrulation and muscle degeneration encodes gelsolin-like and leucine-rich repeat domains and is conserved in *Caenorhabditis elegans* and humans. Proc. Natl. Acad. Sci. USA *90*, 11386–11390.

Celis, J.E. (ed.) (1994). Cell Biology: A Laboratory Manual, San Diego: Academic Press.

Claviez, M., Pagh, K., Maruta, H., Baltes, W., Fisher, P., and Gerisch, G. (1982). Electron microscopic mapping of monoclonal antibodies on the tail region of *Dictyostelium* myosin. EMBO J. *1*, 1017–1022.

D'Haese, J., and Hinssen, H. (1987). Isolation and characterization of a calcium-activated actin-modulating protein from obliquely striated muscle. J. Comp. Physiol. B *157*, 615–623.

Desjardins, M., Celis, J.E., van Meer, G., Dieplinger, H., Jahraus, A., Griffiths, G., and Huber, L.A. (1994). Molecular characterization of phagosomes. J. Biol. Chem. *23*, 32194–32200.

Eddy, R.J., Han, J., and Condeelis, J.S. (1997). Capping protein terminates but does not initiate chemoattractant-induced actin assembly in *Dictyostelium*. J. Cell. Biol. *139*, 1243–1253.

Eichinger, L., and Schleicher, M. (1992). Characterization of actin- and lipid-binding domains in severin, a Ca^{2+}-dependent F-actin fragmenting protein. Biochemistry *31*, 4779–4787.

Feit, I.N., and Sollitto, R.B. (1987). Ammonia is the gas used for the spacing of fruiting bodies in the cellular slime mold *Dictyostelium discoideum*. Differentiation *33*, 193–196.

Fisher, P.R. (1997). Genetics of phototaxis in a model eucaryote. *Dictyostelium discoideum*. Bioessays *19*, 397–407.

Fisher,. P.R., Noegel, A.A., Fechheimer, M., Rivero, F., Prassler, J., and Gerisch, G. (1997). Photosensory and thermosensory responses in *Dictyostelium* slugs are specifically impaired by absence of the F-actin cross-linking gelation factor (ABP-120). Curr. Biol. *7*, 889–892.

Furukawa, R., Butz, S., Fleischmann, E., and Fechheimer, M. (1992). The *Dictyostelium discoideum* 30,000 dalton protein contributes to phagocytosis. Protoplasma *169*, 18–27.

Gerisch, G. (1987). Cyclic AMP and other signals controlling cell development and differentiation in *Dictyostelium*. Annu. Rev. Biochem. *56*, 853–879.

Glenney, J.R., and Weber, K. (1981). Calcium control of microfilaments: uncoupling of the F-actin severing and bundling activity of villin by limited proteolysis in vitro. Proc. Natl. Acad. Sci. USA *78*, 2810–2814.

Goode, B.L., Drubin, D.G., and Lappalainen, P. (1998). Regulation of the cortical actin cytoskeleton in budding yeast by twinfilin, a ubiquitous actin monomer-sequestering protein. J. Cell Biol. *142*, 723–733.

Han, J., Eddy, R.J., and Condeelis, J.S. (1997). Stimulated actin polymerization results from exposure of barbed ends by severing in *Dictyostelium*. Mol. Biol. Cell *7*(suppl), 1479.

Hartmann, H., Schleicher, M., Eckerskorn, C., Rapp, S., and Noegel, A.A. (1989). Ca^{2+}-independent F-actin capping proteins: cap32/34, a capping protein from *Dictyostelium discoideum*, does not share sequence homologies with known actin-binding proteins. J. Biol. Chem. *264*, 12639–12647.

Hasegawa, T., Takahashi, S., Hayashi, H., and Hatano, S. (1980). Fragmin: a calcium ion sensitive regulatory factor on the formation of actin filaments. Biochemistry *19*, 2677–2683.

Heintzelmann, M.B., Frankel, S.A., Artavanis-Tsakonas, S., and Mooseker, M.S. (1993). Cloning of a secretory gelsolin from *Drosophila melanogaster*. J. Mol. Biol. *230*, 709–716.

Hofmann, A. (1994). Isolierung und Charakterisierung von Protovillin, einem neuartigen F-Aktin verkappenden Protein aus *Dictyostelium discoideum*. Ph.D. Thesis. Bayreuth, Germany: Universität Bayreuth.

Hofmann, A., Noegel, A.A., Bomblies, L., Lottspeich, F., and Schleicher, M. (1993). The 100 kDa F-actin capping protein of *Dictyostelium* amoeba is a villin prototype ("protovillin"). FEBS Lett. *328*, 71–76.

Humbel, B.M., and Biegelmann, E. (1992). A preparation protocol for postembedding immunoelectron microscopy of *Dictyostelium discoideum* with monoclonal antibodies. Scanning Mirosc. *6*, 817–825.

Jungbluth, A. (1996). Funktionelle Charakterisierung der Tyrosinphosphorylierung von Actin in *Dictyostelium discoideum*. Ph.D. Thesis. München, Germany: Universität München.

Jungbluth, A., Eckerskorn, C., Gerisch, G., Lottspeich, F., Stocker, S., and Schweiger, A. (1995). Stress-induced tyrosine-phosphorylation of actin in *Dictyostelium* cells and localization of the phosphorylation site to tyrosine-53 adjacent to the DNaseI binding loop. FEBS Lett. *375*, 87–90.

Karlin, S. (1995). Statistical significance of sequence patterns in proteins. Curr. Opin. Struct. Biol. *5*, 360–371.

Kwiatkowski, D.J., Janmey, P.A., Mole, J.E., and Yin, H.L. (1985). Isolation and properties of two actin-binding domains in gelsolin. J. Biol. Chem. *260*, 15232–15238.

Kwiatkowski, D.J., Janmey, P.A., and Yin, H.L. (1989). Identification of critical functional and regulatory domains in gelsolin. J. Cell Biol. *108*, 1717–1726.

Kwiatkowski, D.J., Mehl, R., Izumo, S., Nadal, G.B., and Yin, H.L. (1988a). Muscle is the major source of plasma gelsolin. J. Biol. Chem. *263*, 8239–8243.

Kwiatkowski, D.J., Mehl, R., and Yin, H.L. (1988b). Genomic organization and biosynthesis of secreted and cytoplasmic forms of plasma gelsolin. J. Cell Biol. *106*, 375–384.

Kwiatkowski, D.J., Stossel, T.P., Orkin, S.H., Mole, J.E., Colten, H., and Yin, H.L. (1986). Plasma and cytosolic gelsolins are encoded by a single gene and contain a duplicated actin binding domain. Nature *323*, 455–458.

Kuznetsov, S.A., Langford, G.M., and Weiss, D.G. (1992). Actin-dependent organelle movement in squid axoplasm. Nature *356*, 722–725.

Laemmli, U.K. (1970). Cleavage of structural proteins during the assembly of the head of bacteriophage T4. Nature *227*, 680–685.

Lien, L.L., Feener, C.A., Fischbach, N., Kunkel, L.M. (1994). Cloning of human microtubule-associated protein 1B and the identification of a related gene on chromosome 15. Genomics *22*, 273–280.

Lück, A., D'Haese, J., and Hinssen, H. (1995). A gelsolin-related protein from lobster muscle: cloning, sequence analysis and expression. Biochem J. *305*, 767–775.

Lupas, A. (1996). Coiled coils: new structures and new functions. Trends Biochem. Sci. *21*, 375–382.

Lupas, A., VanDyke, M., and Stock, J. (1991). Predicting coiled coils from protein sequences. Science *252*, 1162–1164.

Maekawa, S., Toriyama, M., Hisanaga, S.-I., Yonezawa, N., Endo, S., Hirokawa, N., and Sakai, H. (1989). Purification and characteriza-

tion of a Ca^{2+}-dependent actin filament severing protein from bovine adrenal medulla. J. Biol. Chem. *264*, 7458–7465.

Marriott, G. (1994). Caged protein conjugates and light-directed generation of protein activity: preparation, photoactivation, and spectroscopic characterization of caged G-actin conjugates. Biochemistry *33*, 9092–9097.

Marsh, J.L., Erfle, M., and Wykes, E.J. (1984). The pIC plasmid and phage vectors with versatile cloning sites for recombinant selection by insertional inactivation. Gene *32*, 481–485.

McGough, A., Chiu, W., and Way, M. (1998). Determination of the gelsolin binding site on F-actin: implications for severing and capping. Biophys. J. *74*, 764–772.

McLaughlin, P.J., Gooch, J.T., Mannherz, H.-G., and Weeds, A.G. (1993). Structure of gelsolin segment 1-actin complex and the mechanism of filament severing. Nature *364*, 685–692.

Muallem, S., Kwiatkowska, K., Xu, X., and Yin, H.L. (1995). Actin filament disassembly is a sufficient final trigger for exocytosis in nonexcitable cells. J. Cell Biol. *128*, 589–598.

Müller, K., and Gerisch, G. (1987). A specific glycoprotein as the target site of adhesion blocking Fab in aggregating *Dictyostelium* cells. Nature *274*, 445–449.

Myers, M.W., Lazzarini, R.A., Lee, V.M.Y., Schlaepfer, W.W., and Nelson, D.L. (1987). The human midsize neurofilament subunit: a repeated protein sequence and the relationship of its gene to the intermediate filament gene family. EMBO J. *6*, 1617–1626.

Newell, P.C., Telser, A., and Sussman, M. (1969). Alternative developmental pathways determined by environmental conditions in the cellular slime mold *Dictyostelium discoideum*. J. Bacteriol. *100*, 763–768.

Noegel, A.A., Harloff, C., Hirth, P., Merkl, R., Modersitzki, M., Stadler, J., Weinhart, U., Westphal, M., and Gerisch, G. (1985). Probing an adhesion mutant of *Dictyostelium discoideum* with cDNA clones and monoclonal antibodies indicates a specific defect in the contact site A glycoprotein. EMBO J. *4*, 3805–3810.

Novy, R.E., Lin, J.L., and Lin, J.J. (1991). Characterization of cDNA clones encoding a human fibroblast caldesmon isoform and analysis of caldesmon expression in normal and transformed cells. J. Biol. Chem. *266*, 16917–16924.

Pestonjamasp, K.N., Pope, R.P., Wulfkuhle, J.D., and Luna, E. (1997). Supervillin (p205). A novel membrane-associated, F-actin binding protein in the Villin/Gelsolin superfamily. J. Cell Biol. *139*, 1255–1269.

Pope, B., Maciver, S., and Weeds, A. (1995). Localization of the calcium-sensitive actin monomer binding site in gelsolin to segment 4 and Identification of calcium binding sites. Biochemistry *34*, 1583–1588.

Prassler, J., Murr, A., Stocker, S., Faix, J., Murphy, J., and Marriott, G. (1998). DdLIM is a cytoskeleton-associated protein involved in the protrusion of lamellipodia in *Dictyostelium*. Mol. Biol. Cell *9*, 545–559.

Prassler, J., Stocker, S., Marriott, G., Heidecker, M., Kellermann, J., and Gerisch, G. (1997). Interaction of a *Dictyostelium* member of the plastin/fimbrin family with actin filaments and actin-myosin complexes. Mol. Biol. Cell *8*, 83–95.

Prendergast, G.C., and Ziff, E.B. (1991). MbhI: a novel gelsolin/severin-related protein which binds actin in vitro and exhibits nuclear localization in vivo. EMBO J. *10*, 757–766

Robbens, J., Louahed, J., Depestel, K., Vancolen, I., Ampe, C., Vandekerckhove, J., and Renauld, J.C. (1998). Murine adseverin (D5), a novel member of the gelsolin family, and murine adseverin are induced by interleukin-9 in T-helper lymphocytes. Mol. Cell. Biol. *18*, 4589–4596.

Sambrook, J., Fritsch, E.F., and Maniatis, T. (1989). Molecular Cloning: A Laboratory Manual, 2nd ed., Cold Spring Harbor, NY: Cold Spring Harbor Laboratory.

Sanger, F., Nicklen, S., and Coulson, A.R. (1977). DNA sequencing with chain terminating inhibitors. Proc. Natl. Acad. Sci. USA *74*, 5463–5468.

Schindler, J., and Sussman, M. (1977). Ammonia determines the choice of morphogenetic pathways in *D. discoideum*. J. Mol. Biol. *28*, 545–554.

Schneider, N., Schwartz, J.-M., and Gerisch, G. (1998). Golgi dynamics visualized by golvesin tagged with GFP. 100th Anniversary Conference: The Golgi Complex, Pavia, Italy, 116.

Scholz, A., and Hinssen, H. (1995). Biphasic pattern of gelsolin expression and variations in gelsolin-actin interactions during myogenesis. Exp. Cell Res. *219*, 384–391.

Simon, M.-N., Mutzel, R., and Veron, M. (1988). Vectors for expression of truncated coding sequences in *E. coli*. Plasmid *19*, 94–102.

Simpson, P.A., Spudich, J.A., and Parham, P. (1984). Monoclonal antibodies prepared against *Dictyostelium* actin: characterization and interactions with actin. J. Cell Biol. *99*, 287–295.

Southwick, F.S., and DiNubile, M. (1986). Rabbit alveolar macrophages contain a Ca²⁺-sensitive, 41,000 Dalton protein which reversibly blocks the "barbed" ends of actin filaments but does not sever them. J. Biol. Chem. *261*, 14191–14195.

Sun, H.-Q., Wooten, D.C., Janmey, P.A., and Yin, H.L. (1994). The actin side-binding domain of gelsolin also caps actin filaments. Implications for actin filament severing. J. Biol. Chem. *269*, 9473–9479.

Sutoh, K. (1993). A transformation vector for *Dictyostelium discoideum* with a new selectable marker bsr. Plasmid *30*, 150–154.

Towbin, H., Staehelin, T., and Gordon, J. (1979). Electrophoretic transfer of proteins from polyacrylamide gels to nitrocellulose sheets: procedure and some applications. Proc. Natl. Acad. Sci. USA *76*, 4350–4354.

van Deurs, B., Holm, P.K., Kayser, L., and Sandvig, K. (1995). Delivery to lysosomes in the human carcinoma cell line HEp-2 involves an actin filament-facilitated fusion between mature endosomes and preexisting lysosomes. Eur. J. Cell Biol. *66*, 309–323

Van Troys, M., Dewitte, D., Goethals, M., Vandekerckhove, J., and Ampe, C. (1996). Evidence for an actin binding helix in gelsolin segment 2: have homologous sequences in segments 1 and 2 of gelsolin evolved to divergent actin binding functions? FEBS Lett. *397*, 191–196.

Van Troys, M., Dewitte, D., Verschelde, J.-L., Goethals, M., Vandekerckhove, J., and Ampe, C. (1997). Analogous F-actin binding by cofilin and gelsolin segment 2 substantiates their structural relationship. J. Biol. Chem. *272*, 32750–32758.

Wallraff, E. (1997). Migration and bidirectional phototaxis in *Dictyostelium discoideum* slugs lacking the actin cross-linking 120 kDa gelation factor. J. Exp. Biol. *200*, 3213–3220.

Wallraff, E., and Gerisch, G. (1991). Screening for *Dictyostelium* mutants defective in cytoskeletal proteins by colony immunoblotting. Methods Enzymol. *196*, 334–348.

Wang, J.S., Coburn, J.P., Tauber, A.I., and Zaner, K.S. (1997). Role of gelsolin in actin depolymerization of adherent human neutrophils. Mol. Biol. Cell *8*, 121–128.

Watts, R.G., Deaton, J.D., and Howard, T.H. (1995). Dynamics of Triton-insoluble and Triton-soluble F-actin pools in calcium-activated human polymorphonuclear leukocytes: evidence for regulation by gelsolin. Cell Motil. Cytoskeleton *30*, 136–145.

Way, M., Gooch, J., Pope, B., and Weeds, A.G. (1989). Expression of human plasma gelsolin in *Escherichia coli* and dissection of actin binding sites by segmental deletion mutagenesis. J. Cell Biol. *109*, 593–605.

Way, M., and Weeds, A. (1988). Nucleotide sequence of pig plasma gelsolin. Comparison of protein sequence with human gelsolin and other actin-severing proteins shows strong homologies and evidence for large internal repeats. J. Mol. Biol. *203*, 1127–1133.

Weeds, A., and Maciver, S. (1993). F-actin capping proteins. Curr. Opin. Cell Biol. *5*, 63–69.

Weber, A., Pring, M., Lin, S.-L., and Bryan, J. (1991). Role of the N- and C-terminal actin-binding domains of gelsolin in barbed filament end capping. Biochemistry *30*, 9327–9334.

Williams, G.B., Elder, E.M., and Sussman, M. (1984). Modulation of the cAMP relay in *Dictyostelium discoideum* by ammonia and other metabolites: possible morphogenetic consequences. Dev. Biol. *105*, 377–388.

Yamamoto, K., Pardee, J.D., Reidler, J., Stryer, L., and Spudich, J.A. (1982). Mechanism of interaction of *Dictyostelium* severin with actin filaments. J. Cell Biol. *95*, 711–719.

Yin, H.L., and Stossel, T.P. (1979). Control of cytoplasmic actin gel-sol transformation by gelsolin, a calcium-dependent regulatory protein. Nature *281*, 583–586.

Yu, F.-X., Sun, H.-W., Janmey, P.A., and Yin, H.L. (1992). Identification of a polyphosphatidylinositide-binding sequence in an actin-monomer-binding domain of gelsolin. J. Biol. Chem. *267*, 14616–14621.